J|A|C|S
ARTICLES

Self-Assembly of Dendronized Triphenylenes into Helical Pyramidal Columns and Chiral Spheres

Virgil Percec,[*,†] Mohammad R. Imam,[†] Mihai Peterca,[†,‡] Daniela A. Wilson,[†]
Robert Graf,[§] Hans W. Spiess,[§] Venkatachalapathy S. K. Balagurusamy,[†] and
Paul A. Heiney[‡]

Roy & Diana Vagelos Laboratories, Department of Chemistry, University of Pennsylvania, Philadelphia, Pennsylvania 19104-6323, Department of Physics and Astronomy, University of Pennsylvania, Philadelphia, Pennsylvania 19104-6396, and Max-Planck Institute for Polymer Research, 55128 Mainz, Germany

Received December 4, 2008; E-mail: percec@sas.upenn.edu

Abstract: The synthesis and structural and retrostructural analyses of a library containing 10 triphenylenes functionalized with self-assembling benzyl ether and phenyl propyl ether dendrons are reported. These dendronized triphenylenes adopt a crown rather than discotic conformation. Their crown conformation mediates the self-assembly of the discotic triphenylene unit in helical pyramidal columns and in chiral spheres. The chiral spheres are generated from short segments of helical pyramidal columns that are spherically distorted. Therefore, the chirality of the sphere is determined by a short helical pyramidal column that represents the inner part of the supramolecular sphere. Both the helical pyramidal columns and the chiral spheres represent supramolecular architectures that were self-assembled for the first time from discotic molecules. The helical pyramidal columns self-organize in various hexagonal and rectangular lattices, while the chiral spheres self-organize into cubic and tetragonal periodic arrays and into a quasiperiodic 12-fold liquid quasicrystal. The helical sense of the helical pyramidal columns and of helical spheres is selected by a stereocenter that can be incorporated either in the alkyl groups of the dendron or in the triphenylene part of the dendritic crown via donor−acceptor interactions. The self-assembly process of the dendronized triphenylene donor can be programmed by a new supramolecular "polymer effect" generated by donor−acceptor interactions.

Introduction

Disc-like molecules functionalized with alkyl groups self-assemble into supramolecular columns that self-organize into hexagonal, rectangular, and nematic phases most frequently referred to as discotic or columnar liquid crystals.[1] Hexasubstituted triphenylenes[1b,c] are some of the most widely investigated self-assembling disc-like molecules, although different architectures and larger shapes were also elaborated.[2,3] Macroscopic evidence of molecular chirality in columnar mesophases was first observed in triphenylenes containing stereocenters in their alkyl groups.[4] However, it was the discovery of high charge carrier mobility in a helical columnar structure derived from a nonchiral triphenylene derivative that generated an enormous interest in the semiconducting, photoconducting, and other electronic properties of columnar liquid crystal materials.[5] Supramolecular assemblies related to those produced from disc-like molecules are also obtained by the self-assembly of tapered dendrons[6] into supramolecular columns and their self-organization into various columnar lattices. Some of the supramolecular columns generated by self-assembling tapered dendrons are helical.[6]

The molecular structure of a library of columnar supramolecular dendrimers that are helical was recently elucidated.[7] That

---

[†] Department of Chemistry, University of Pennsylvania.

[‡] Department of Physics and Astronomy, University of Pennsylvania.

[§] Max-Planck Institute for Polymer Research.

(1) For pioneering publications on discotic liquid crystals, see: (a) Chandrasekhar, S.; Sadashiva, B. K.; Suresh, K. A *Pramana* **1977**, *9*, 471–480. (b) Billard, J.; Dubois, J. C.; Nguyen, H. T.; Zann, A *Nouv. J. Chim* **1978**, *2*, 535–540. (c) Destrade, C.; Mondon, M. C.; Malthête, J. *J. Phys. (Paris)* **1979**, *3*, 17–21.

(2) For selected reviews and recent publications on discotic liquid crystals, see: (a) Watson, M. D.; Fechtenkötter, A.; Müllen, K. *Chem. Rev.* **2001**, *101*, 1267–1300. (b) Bushby, R. J.; Lozman, O. R. *Curr. Opin. Colloid Interface Sci.* **2002**, *7*, 343–354. (c) Bushby, R. J.; Lozman, O. R. *Curr. Opin. Solid State Mater. Sci.* **2002**, *6*, 569–378. (d) Sergeyev, S.; Pisula, W.; Geerts, Y. H. *Chem. Soc. Rev.* **2007**, *36*, 1902–1929. (e) Motoyanagi, J.; Fukushima, T.; Aida, T. *Chem. Commun.* **2005**, 101–103. (f) Goodby, J. W.; Hird, M.; Toyne, K. J.; Watson, T. *J. Chem. Soc., Chem. Commun.* **1994**, 1701–1702. (g) Reichert, A.; Ringsdorf, H.; Schuhmacher, P.; Baumeister, W.; Scheybani, T. In *Comprehensive Supramolecular Chemistry*; Lehn, J. M., Ed.; Pergamon: New York, 1996; Vol. 9, pp 313−350. (h) Würthner, F. *Chem. Commun.* **2004**, 1564–1579. (i) de Frutos, O.; Gómez-Lor, B; Granier, T.; Monge, M. A.; Gutierrez-Puebla, E.; Echavarren, A. M. *Angew. Chem., Int. Ed.* **1999**, *38*, 204–207.

(3) (a) Arikainen, E. O.; Boden, N.; Bushby, R. J.; Lozman, O. R.; Vinter, J. G.; Wood, A. *Angew. Chem., Int. Ed.* **2000**, *39*, 2333–2336. (b) Feng, X.; Pisula, W.; Zhi, L.; Takase, M.; Müllen, K. *Angew. Chem., Int. Ed.* **2008**, *47*, 1703–1706. (c) Lehmann, M.; et al. *Chem.-Eur. J.* **2005**, *11*, 3349–3362. (d) Bao, Z.; Lovinger, A. J.; Brown, J. *J. Am. Chem. Soc.* **1998**, *120*, 207–208. (e) Ochsenfeld, C.; Brown, S. P.; Schnell, I.; Gauss, J.; Spiess, H. W. *J. Am. Chem. Soc.* **2001**, *123*, 2597–2606. (f) Engelkamp, H.; Middelbeek, S.; Nolte, R. J. M. *Science* **1999**, *284*, 785–788. (g) Garcia-Frutos, E. M.; Gómez-Lor, B *J. Am. Chem. Soc.* **2008**, *130*, 9173–9177.

10.1021/ja8094944 CCC: $40.75

Scheme 1. Dendronized Triphenylene (Tp) Derivatives

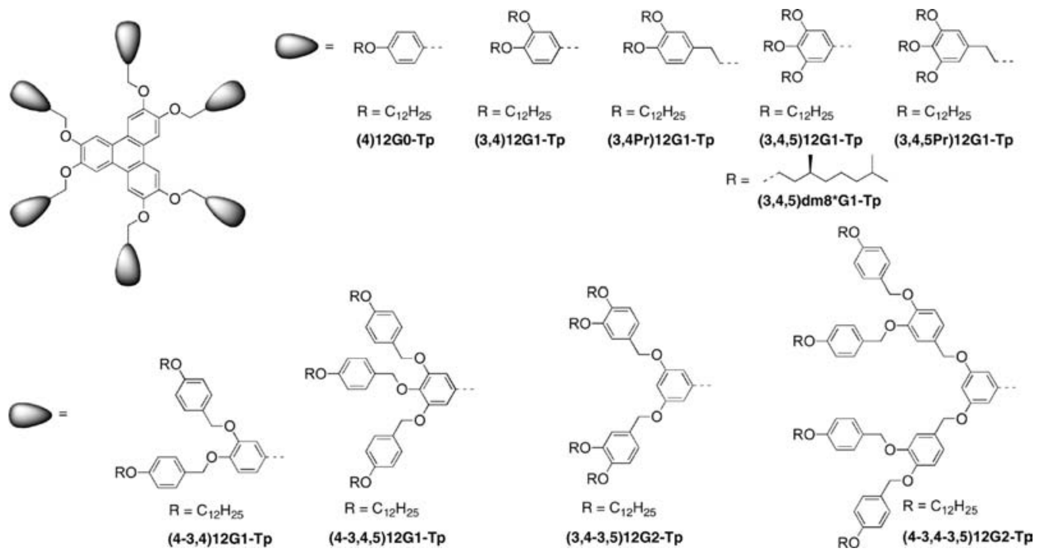

investigation discovered that a crown conformation that can be exhibited by dendrons, dendrimers, and supramolecular dendrimers, which we named *dendritic crown*, provides a new strategy in the design of helical pyramidal columns with various supramolecular architectures.[7] Helical pyramidal columns were previously assembled only from conformationally rigid molecular crowns such as cyclotriveratrylene.[8] As mathematically described, a sphere cannot be chiral. However, rigid models of crowns obtained from dendronized cyclotriveratrylene were recently reported to self-assemble also into chiral supramolecular spheres[9a] that self-organize into $Pm\bar{3}n$ cubic[10a] and $P4_2/mnm$ tetragonal[10b] lattices. These chiral spheres are generated from short segments of helical pyramidal columns that are spherically distorted. Therefore, the chirality of these spheres is determined by their internal helical structure,[9a] as was the case in other examples of chiral supramolecular spherical dendrimers.[9b] Molecular engineering of more complex structures based on disc-like molecules by the group of Aida mediated their assembly into the first noncolumnar structures.[11]

This publication reports the functionalization of triphenylene with self-assembling dendrons. The resulting dendronized triphenylenes exhibit a crown conformation and self-assemble into helical pyramidal columns and chiral spheres. The helical pyramidal columns self-organize in various columnar hexagonal and rectangular lattices, while the chiral spheres self-organize into periodic $Pm\bar{3}n$ cubic,[10a] $P4_2/mnm$ tetragonal,[10b] and 12-fold liquid quasicrystal (LQC) quasiperiodic[12] arrays. Donor−acceptor interactions were shown to program the shape of the supramolecular structures assembled from dendronized triphenylene donor via a supramolecular "polymer effect". This diversity of new supramolecular architectures generated from dendronized triphenylene via their unprecedented crown conformation is expected to be general for all classes of dendronized disc-like molecules and, therefore, will expand the supramolecular structures in which discotic molecules self-assemble.

Results and Discussion

Dendronized Triphenylenes (Tp) with Directly Attached Self-Assembling Benzyl Ether and Phenyl Propyl Ether Dendrons. Ten dendronized triphenylenes (Tp) were synthesized. Scheme 1 illustrates the structures of the triphenylenes

---

(4) Malthête, J.; Jacques, J.; Tinh, N. H.; Destrade, C. *Nature (London)* **1982**, *298*, 46–48.

(5) (a) Adam, D.; Schuhmacher, P.; Simmerer, J.; Häussling, L.; Siemensmeyer, K.; Etzbachi, K. H.; Ringsdorf, H.; Haarer, D. *Nature (London)* **1994**, *371*, 141–143. (b) Adam, D.; Closs, F.; Frey, T.; Funhoff, D.; Haarer, D.; Ringsdorf, H.; Schuhmacher, P.; Siemensmeyer, K. *Phys. Rev. Lett.* **1993**, *70*, 457–460. (c) Arikainen, E. O.; Boden, N.; Bushby, R. J.; Clements, J.; Movaghar, B.; Wood, A. *J. Mater. Chem.* **1995**, *5*, 2161–2165.

(6) For selected examples of supramolecular columns from self-assembling tapered dendrons see: (a) Percec, V.; Cho, W. D.; Ungar, G.; Yeardley, D. J. P. *J. Am. Chem. Soc.* **2001**, *123*, 1302–1315. (b) Percec, V.; Dulcey, A. E.; Balagurusamy, V. S. K.; Miura, Y.; Smidrkal, J.; Peterca, M.; Nummelin, S.; Edlund, U.; Hudson, S. D.; Heiney, P. A.; Hu, D. A.; Magonov, S. N.; Vinogradov, S. A. *Nature (London)* **2004**, *430*, 764–768. (c) Hudson, S. D.; Jung, H.-T.; Percec, V.; Cho, W. D.; Johansson, G.; Ungar, G.; Balagurusamy, V. S. K. *Science* **1997**, *277*, 449–452. (d) Percec, V.; Won, B. C.; Peterca, M.; Heiney, P. A. *J. Am. Chem. Soc.* **2007**, 11265–11278. (e) Percec, V.; Dulcey, A. E.; Peterca, M.; Ilies, M.; Nummelin, S.; Sienkowska, M. J.; Heiney, P. A. *Proc. Natl. Acad. Sci. U.S.A.* **2006**, *103*, 2518–2523. (f) Cho, B.-K.; Jain, A.; Gruner, S. M.; Wiesner, U. *Science* **2004**, *305*, 1598–1601. (g) Suarez, M. I.; Lehn, J.-M.; Zimmerman, S. C.; Skoulios, A.; Heinrich, B. *J. Am. Chem. Soc.* **1998**, *120*, 9526–9532. (h) Donnio, B.; Guillon, D. *Adv. Polym. Sci.* **2006**, *201*, 45–155. (i) Guillon, D.; Deschenaux, R *Curr. Opin. Solid State Mater. Sci* **2002**, *6*, 515–525.

(7) Peterca, M.; Percec, V.; Imam, M. R.; Leowanawat, P.; Morimitsu, K.; Heiney, P. A. *J. Am. Chem. Soc.* **2008**, *130*, 14840–14852.

(8) (a) Collet, A. In *Comprehensive Supramolecular Chemistry*; Atwood, J. L., Davies, J. E. D.; MacNicol, D. D., Vögtle, F., Eds.; Pergamon: New York, 1996; Vol. 6, pp 281−303. (b) Collet, A. *Tetrahedron* **1987**, *43*, 5725–5759. (c) Malthête, J.; Collet, A. *Nouv. J. Chim* **1985**, *9*, 151–153. (d) Zimmermann, H.; Poupko, R.; Luz, Z.; Billard, J. *Z. Naturforsch.* **1985**, *40a*, 149–160. (e) Malthête, J.; Collet, A. *J. Am. Chem. Soc.* **1987**, *109*, 7544–7545. (f) Poupko, R.; Luz, Z.; Spielberg, N.; Zimmermann, H. *J. Am. Chem. Soc.* **1989**, *111*, 6094–6105. (g) Lesot, P.; Merlet, D.; Sarfati, M.; Courtieu, J.; Zimmermann, H.; Luz, Z. *J. Am. Chem. Soc.* **2002**, *124*, 10071–10082. (h) Zimmermann, H.; Bader, V.; Poupko, R.; Wachtel, E. J.; Luz, Z. *J. Am. Chem. Soc.* **2002**, *124*, 15286–15301. (i) Levelut, A. M.; Malthête, J.; Collet, A. *J. Phys. (Paris)* **1986**, *47*, 351–357.

(9) (a) Percec, V.; Imam, M. R.; Peterca, M.; Wilson, D. A.; Heiney, P. A. *J. Am. Chem. Soc.* **2009**, *131*, 1294–1304. (b) Percec, V.; Peterca, M.; Dulcey, A. E.; Imam, M. R.; Hudson, S. D.; Numnelin, S.; Adelman, P.; Heiney, P. A. *J. Am. Chem. Soc.* **2008**, *130*, 13079–13094.

(10) (a) Balagurusamy, V. S. K.; Ungar, G.; Percec, V.; Johansson, G. *J. Am. Chem. Soc.* **1997**, *119*, 1539–1555. (b) Ungar, G.; Liu, Y. S.; Zeng, X. B.; Percec, V.; Cho, W. D. *Science* **2003**, *299*, 1208–1211.

(11) Hill, J. P.; Jin, W.; Kosaka, A.; Fukushima, T.; Ichihara, H.; Shimomura, T.; Ito, K.; Hashizume, T.; Ishii, N.; Aida, T. *Science* **2004**, *304*, 1481–1483.

(12) Zeng, X. B.; Ungar, G.; Liu, Y. S.; Percec, V.; Dulcey, S. E.; Hobbs, J. K. *Nature (London)* **2004**, *428*, 157–160.

Table 1. Thermal Analysis of the 2-D and 3-D Lattices Self-Organized from the Supramolecular Dendrimers Self-Assembled from Dendronized Triphenylenes

	thermal transitions (°C) and corresponding enthalpy changes (kcal mol^{-1}) ^{a}	
compound	heating	cooling
(4)12G1-Tp	g 86.0 (23.01) Φ_h^{io} 159.1 (1.31) i g 86.1 (2.32) X 93.2 (1.06) Φ_h^{io} 157.6 (1.19) i	i 155.4 (−1.13) Φ_h^{io} 74.8 (−5.49) g
(3,4)12G1-Tp	k 50.9 (16.25) Φ_h^{io} 143.6 (2.23) i $\Phi_h^{crystal}$ 18.1 (10.83) Φ_h^{io} 142.9 (2.09) i	i 140.9 (−2.06) Φ_h^{io} 10.8 (−8.35) $\Phi_h^{crystal}$
(3,4Pr)12G1-Tp	k 60.6 (52.25) Φ_h 114.2 (7.47) i Φ_h^{io-1} 31.2 (18.99) Φ_h^{io-2} 57.8 (2.08) Φ_h 114.3 (7.25) i	i 112.4 (−7.18) Φ_h 23.8 (−17.65) Φ_h^{io}
(4-3,4)12G1-Tp	g −11.1 (13.20) Φ_h^{io} 247.8 (4.69) i g −7.3 (14.90) Φ_h^{io} 238.3 (4.27) i	i 235.9 (−5.0) Φ_h^{io}
(3,4,5)12G1-Tp	$\Phi_h^{crystal}$ 6.5 (9.89) Φ_h 38.5 (1.57) *Tet* 80.0 *Cub*^{b} 104.8 (0.91) i $\Phi_h^{crystal}$ 6.5 (9.62) Φ_h 39.6 (1.52) *Tet* 80.0 *Cub*^{b} 104.7 (0.85) i	i 91.5 (−0.31) *Cub* 66.0 (−0.13) *Tet* 23.8 (−1.57) Φ_h −0.5 (−12.42) $\Phi_h^{crystal}$
(3,4,5Pr)12G1-Tp	k 15.5 (13.84) Φ_h^{io} 35.4 (6.91) X 43.1(1.57) i $\Phi_{r\text{-}c}^{crystal}$ 15.4 (12.12) Φ_h^{io} 35.5 (5.93) i	i 30.2 (−7.21) Φ_h^{io} 9.0 (−11.56) $\Phi_{r\text{-}c}^{crystal}$
(3,4,5)dm8*12G1-Tp	*Tet* 55.1 (1.97) *Cub* 84.5 (1.08) i *Tet* 55.2 (1.99) *Cub* 84.3 (1.12) i	i 64.4 (−0.30) *Cub* 37.8 (−2.19) *Tet*
(4-3,4,5)12G1-Tp	k −20.9 (16.75) Φ_h^{io} 126.0 (1.83) i $\Phi_h^{crystal}$ −16.9 (22.35) Φ_h^{io} 125.6 (1.80) i	i 120.5 (−2.48) Φ_h^{io} −24.2 (−40.73) $\Phi_h^{crystal}$
(3,4-3,5)12G2-Tp	Φ_h 38.6 LQC 136.1 (0.44) *Cub* 148.4 (2.57) i Φ_h 77.0 LQC 134.0 (0.25) *Cub* 148.1 (2.17) i	i 141.3 (−1.50) *Cub* 114.7 (−0.31) LQC 81.1 (−2.35) Φ_h
(4-3,4-3,5)12G2-Tp	g 46.3 (1.22) Φ_h^{io} 154.0 (6.28) *Tet* 203.2 (0.003) LQC 214.2 (4.71) i Φ_h^{io} 162.8 (8.22) *Tet* 200.0 (0.11) LQC 211.1 (4.10) i	i 206.1 (−2.95) LQC 178.3 (0.52) *Tet* 133.7 (−2.91) Φ_h^{io}

[a] Data obtained from the first heating and cooling DSC scans are on the first line, and data from the second heating are on the second line for each compound. g, glassy phase; Φ_h^{io}, columnar hexagonal lattice with intracolumnar order; X, mixed phased; i, isotropic; k, crystalline; Φ_h, $p6mm$ hexagonal columnar lattice; $\Phi_h^{crystal}$, crystal hexagonal columnar lattice; *Cub*, $Pm\bar{3}n$ cubic lattice; *Tet*, $P4_2/mnm$ tetragonal lattice; $\Phi_{r\text{-}c}^{crystal}$, crystal-centered rectangular columnar lattice; $\Phi_{r\text{-}c}$, $c2mm$ centered rectangular columnar lattice; and LQC, liquid quasi crystal. [b] Phase observed only by XRD.

dendronized with self-assembling benzyl ether[6a] and phenylpropyl ether[13c] dendrons attached directly to the triphenylene unit. Their synthesis and analytical data are available in the Supporting Information. The thermal analysis of the supramolecular structures self-assembled from these dendronized triphenylenes was carried out by a combination of differential scanning calorimetry (DSC), thermal optical polarized microscopy (TOPM), and X-ray diffraction (XRD) experiments. Powder and fiber small- and wide-angle XRD experiments were used to determine the lattices in which the supramolecular dendrimers are self-organized.

Table 1 summarizes the results obtained by this combination of methods. **(4)12G0-Tp**, **(3,4)12G1-Tp**, **(3,4Pr)12G1-Tp**, **(3,4,5Pr)12G1-Tp**, **(4-3,4)12G1-Tp**, and **(4-3,4,5)12G1-Tp** self-assemble into supramolecular columns that self-organize in a 2-D hexagonal columnar lattice without (Φ_h) and with intracolumnar order (Φ_h^{io}).

The assignment of the phases was made by small- and wide-angle XRD experiments carried out on oriented fibers. At low temperature **(3,4,5)12G1-Tp** shows a crystalline hexagonal columnar phase ($\Phi_h^{crystal}$). On increasing temperature, **(3,4,5)12G1-Tp** exhibits the sequence of phases Φ_h, $P4_2/mnm$ tetragonal, and $Pm\bar{3}n$ cubic (Figure 1).

It is well established that changing the number of methylenic units from the alkyl groups of discotic molecules[5c] and of tapered dendrons[6e,17c,e] frequently maintains a columnar supramolecular assembly over a large number of carbons. The incorporation of a branched stereocenter in the n-alkyl groups at the periphery of **(3,4,5)12G1-Tp** eliminates the formation of the Φ_h phase and the resulting **(3,4,5)dm8*G1-Tp** exhibits only the $P4_2/mnm$ tetragonal and $Pm\bar{3}n$ cubic phases (Figure 2). **(3,4-3,5)12G2-Tp** displays the sequence of phases Φ_h, LQC, and $Pm\bar{3}n$ (Figure 3). **(4-3,4-3,5)12G2-Tp** displays the sequence of phases Φ_h^{io}, $P4_2/mnm$, and 12-fold LQC. An interesting observation of the thermal behavior of **(3,4,5)12G1-Tp** and **(3,4,5)dm8*G1-Tp** dendronized triphenylenes is the occurrence of the $P4_2/mnm$ tetragonal phase at low temperatures and the $Pm\bar{3}n$ cubic phase at high temperatures (Figures 1 and 2). This sequence shows the reverse order of that encountered for the tapered dendrons.[10b] Most probably, the more complex intra- and intermolecular interactions of the crown conformers are responsible for the reverse of the sequence from $\Phi_h \rightarrow Pm\bar{3}n \rightarrow P4_2/mnm$ encountered most frequently, to the current $\Phi_h \rightarrow P4_2/mnm \rightarrow Pm\bar{3}n$ sequence that was observed for the first time here.

Structural and Retrostructural Analysis of Dendronized Tp with Directly Attached Dendrons. Table 2 summarizes the XRD data used to identify the structures reported in Table 1. The data obtained from fiber XRD experiments are reported in

---

(13) (a) Percec, V.; Holerca, M. N.; Nummelin, S.; Morrison, J. J.; Glodde, M.; Smidrkal, J.; Peterca, M.; Rosen, B. M.; Uchida, S.; Balagurusamy, V. S. K.; Sienkowska, M. J.; Heiney, P. A *Chem. -Eur. J* **2006**, *12*, 6216–6241. (b) Percec, V.; Smidrkal, J.; Peterca, M.; Mitchell, C. M.; Nummelin, S.; Dulcey, A. E.; Sienkowska, M. J.; Heiney, P. A *Chem. -Eur. J* **2007**, *13*, 3989–4007. (c) Percec, V.; Peterca, M.; Sienkowska, M. J.; Ilies, M. A.; Aqad, E.; Smidrkal, J.; Heiney, P. A. *J. Am. Chem. Soc.* **2006**, *128*, 3324–3334.

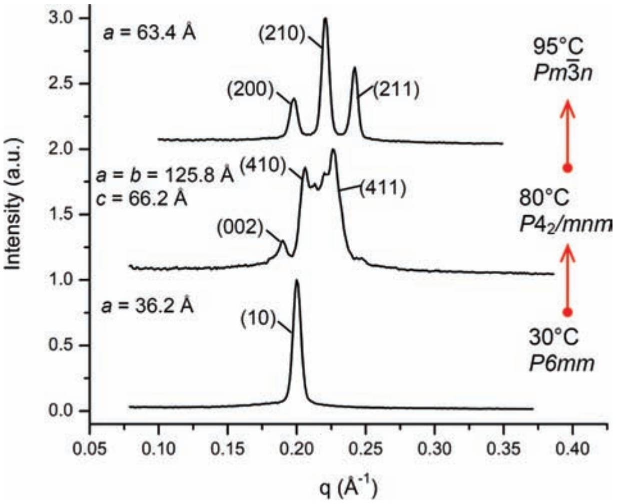

Figure 1. Small-angle XRD powder plots collected for **(3,4,5)12G1-Tp** in the *p*6*mm* columnar hexagonal, *P*4$_2$/*mnm* tetragonal, and *Pm*$\bar{3}$*n* cubic lattices at the indicated temperatures.

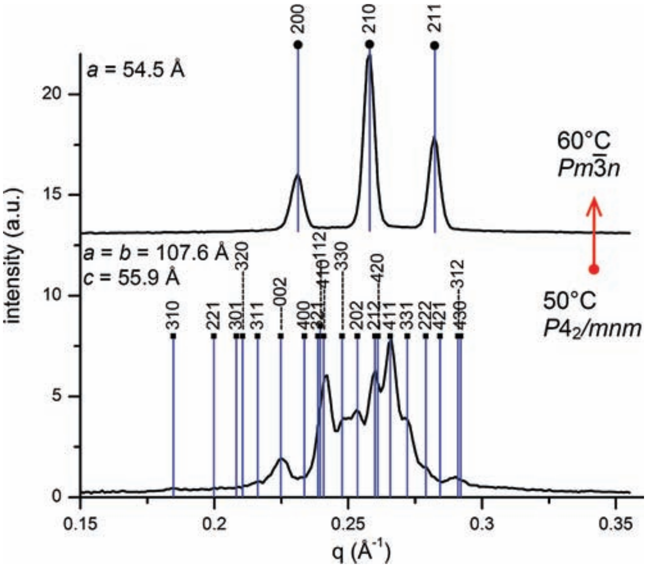

Figure 2. Small-angle XRD powder plots collected for **(3,4,5)dm8*G1-Tp** in the *P*4$_2$/*mnm* tetragonal and *Pm*$\bar{3}$*n* cubic lattices at the indicated temperatures.

Table 3. In the Φ_h phase the lattice dimension *a* is equal to the diameter of the supramolecular column. It is interesting to compare the diameter of **(3,4)12G1-Tp** (48.2 Å) with those of **(3,4,5)12G1-Tp** (37.4 Å), **(4-3,4)12G1-Tp** (50.0 Å), and **(4-3,4,5)12G1-Tp** (48.2 Å). The first two dendronized Tp must have the smallest diameter, since the dendrons attached are first generation. Nevertheless, the experimental data show that **(3,4,5)12G1-Tp** has a smaller diameter as compared with **(3,4)12G1-Tp**. At the same time, the diameter of **(4-3,4)12G1-Tp** is almost equal to that of **(4-3,4,5)12G1-Tp**. Theoretically, if the discotic molecules would adopt a disc-like conformation, the diameters of **(4-3,4)12G1-Tp** and **(4-3,4,5)12G1-Tp** would be equal but larger than the diameter of **(3,4)12G1-Tp**. This discrepancy can be explained only by a tilt of the dendron versus the plane of Tp; therefore, the dendronized Tp must adopt a crown conformation. The tilt values of the crown conformations were determined for five dendronized Tp from their fiber wide- and small-angle XRD and are reported in Table 3. Table 3 also contains the short-range helical pitch and the π-stacking values obtained from fiber XRD experiments. These data also suggest that the dendritic crowns self-assemble in a helical pyramidal column that will be discussed in more detail in a separate section.

(3,4,5)12G1-Tp shows, at 84 °C, a group of seven closely spaced peaks and an isolated weak peak at lower angle that occur at the expected positions from a *P*4$_2$/*mnm* tetragonal phase. The intensity distribution of these peaks is closely related to the previous tetragonal phase.[10b] The peak positions correspond to the lattice dimensions $a = b = 124.0$ Å and $c = 64.8$ Å. As in the previous tetragonal phase,[10b] the *a* and *b* dimensions are nearly double the value of *c*. This suggests that the structures of the tetragonal phases self-organized from dendrons and dendrimers with and without Tp cores are isomorphic. At higher temperatures, as well as on cooling from the isotropic phase, **(3,4,5)12G1-Tp** forms a cubic phase with the space-group symmetry *Pm*$\bar{3}$*n*, showing a characteristic triplet of strong peaks with the indices (200), (210), and (211) and an intensity distribution similar to that of the previously observed *Pm*$\bar{3}$*n* phases. The dimension of this cubic lattice is 65.4 Å, which is almost the same as the *c*-axis dimension of the tetragonal phase. Similar features have been observed in other supramolecular dendrimers, which show both the tetragonal and the cubic phases.[6a,10b] Small-angle XRD patterns recorded from **(3,4-3,5)12G2-Tp** show at 144 °C a triplet of strong peaks that occurs at the expected positions for a *Pm*$\bar{3}$*n* cubic phase with a lattice dimension of $a = 73.1$ Å (Figure 3). The intensity distribution of the peaks in the pattern is very similar to that found for **(3,4,5)12G1-Tp** in the *Pm*$\bar{3}$*n* cubic phase. At 130 °C the XRD pattern shows three closely spaced strong peaks and a weak peak close to this triplet. The peak positions and the relative intensity distribution of the peaks are very similar to the diffraction pattern of the LQC phase.[12]

Finally, **(4-3,4-3,5)12G2-Tp** shows a sequence of phases in the small-angle XRD. On heating at 91 °C, it shows a 2-D Φ_h^{io} phase (Table 2) with a column diameter of 55.1 Å. At 155 °C the (10) peak of the hexagonal phase splits into two closely spaced strong peaks as it slowly transforms to a *P*4$_2$/*mnm* tetragonal phase on further heating. The observed XRD peak positions correspond to the lattice dimensions $a = b = 178.3$ Å and $c = 96.8$ Å. At 203 °C another phase appears with the intensity distribution (Table 2) consistent with that previously assigned to the LQC phase.

Oriented fibers of **(4-3,4-3,5)12G2-Tp**, **(4-3,4,5)12G1-Tp**, **(4-3,4)12G1-Tp**, **(3,4)12G1-Tp**, and **(4)12G0-Tp** were prepared by extrusion in the Φ_h phase[7] and were analyzed by wide-angle and small-angle XRD in the columnar phases. In all cases, wide-angle XRD showed small-angle features with maximum intensity near the equatorial line, indicating preferential alignment of the supramolecular columns along the extrusion direction. Molecular models of **(4-3,4-3,5)12G2-Tp** were built in which the disc-like triphenylene core and the dendron part are flat and untilted with respect to the column axis. In other words, the normal to their molecular plane is parallel to the column axis. In this conformation, the diameter of the molecule was estimated to be nearly 72 Å, with due allowance for the *trans*-gauche isomerization of the C−C bonds in the aliphatic chains of the molecule and assuming that the aliphatic chains of the molecules in the neighboring columns do not interdigitate. This shows that there should be a substantial tilt of the dendron part of the molecule about the column axis. Therefore, dendronized Tp are not disc-like but crown-like, with the dendron tilted with respect to the column axis. The crown-like dendronized Tp self-

Table 2. Structural and Retrostructural Analysis of the Supramolecular Dendrimers Self-Assembled from Dendronized Triphenylene by XRD

			peak *d*-spacings (Å and their indices						
dendrimer	phase	T (°C)	$^a d_{10}$ $^b d_{200}$ $^c d_{310}$ $^d d_{212}$ $^e d_{20}$ $^f d_{00002}$	d_{11} d_{210} d_{002} d_{411} d_{11} d_{12100}	d_{20} d_{211} d_{410} d_{331} d_{31} d_{10102}	d_{330}/d_{202} d_{312} $d_{02}d_{12101}$	lattice dimension or column diameter a $(a, b)^g$ (Å)	D_{sphere} ^{i} (Å)	t ^{j}(Å)	μ^k
(4)12G0-Tp	Φ_h^{io}	120	^{a} 29.5	17.0	–	–	34.1	–	3.6	1.0
(3,4)12G1-Tp	Φ_h^{io}	70	^{a} 41.9	24.0	20.9	–	48.2	–	3.6	1.3
(3,4Pr)12G1-Tp	Φ_h^{io}	30	^{a} 37.8	21.9	19.0	–	43.8	–	3.6	1.0
	Φ_h	80	^{a} 37.0	21.4	18.5	–	42.7	–	–	–
(3,4,5)12G1-Tp	$\Phi_h^{crystal}$	−20	^{a} 32.4	18.7	–	–	37.4	–	4.7	0.8
	Φ_h	25	^{a} 31.4	18.6	–	–	37.0	–	–	–
	Tet	70	^{c} 39.0	32.4	30.1	28.9	$a = b = 124.0$	39.9	–	4.5
			^{d} 27.9	27.3	26.6		$c = 64.8$			
	Cub	84	^{b} 32.7	29.1	26.7	–	65.4	40.5	–	4.4
(3,4,5Pr)-12G1-Tp	$\Phi_{r\text{-}c}{}^h$	**−10**	^{e} 38.5	35.8	21.6	20.2	$a = 76.9$ $b = 40.4$	–	–	–
	Φ_h^{io}	**25**	^{a} 36.9	21.3	18.5	–	42.6	–	4.5	1.0
(3,4,5)dm8*G1-Tp	*Tet*	50	^{c} 34.0	27.9	26.1	25.4/24.8	$a = b = 107.6$	34.5	–	3.5
			^{d} 24.2	23.7	23.1	21.6	$c = 55.9$			
	Cub	60	^{b} 27.3	24.4	22.3	–	54.5	33.8	–	3.3
(4-3,4)12G1-Tp	Φ_h^{io}	155	^{a} 43.3	24.9	21.7	–	50.0	–	3.7	1.0
(4-3,4,5)12G1-Tp	Φ_h^{io}	100	^{a} 41.9	24.0	20.9	–	48.2	–	4.6	0.9
(4-3,4-3,5)12G2-Tp	Φ_h^{io}	91	^{a} 47.6	27.6	23.9	–	55.1	–	4.7	0.8
	Tet	180	^{c} 50.7	48.4	43.2	–	$a = b = 178.3$	58.1	–	6.5
			^{d} 41.4	39.5	36.7		$c = 96.8$			
	LQC	210	^{f} 55.4	51.9	39.9	38.8	–	–	–	–
(3,4-3,5)12G2-Tp	Φ_h	25	^{a} 43.0	–	–	–	49.6	–	4.7	0.9
	LQC	132	^{f} 37.4	34.3	32.7	31.0	–	–	–	–
	Cub	141	^{b} 37.0	33.1	30.2	–	74.0	45.9	–	4.4

[a] *d*-spacings with indices for *p*6*mm* hexagonal columnar lattice (Φ_h). [b] *d*-spacings with indices for $Pm\bar{3}n$ cubic lattice (*Cub*). [c] *d*-spacings with indices for $P4_2/mnm$ tetragonal lattice (*Tet*). [d] *d*-spacings with indices for $P4_2/mnm$ tetragonal lattice (*Tet*). [e] *d*-spacings with indices for *c*2*mm* centered rectangular columnar lattice ($\Phi_{r\text{-}c}$). [f] *d*-spacings with indices for liquid quasicrystal (LQC). [g] For the Φ_h phase lattice dimension, *a* is same as the column diameter. For the $\Phi_{r\text{-}c}$ LC phase lattice dimensions, *a* and *b* are given. For the $P4_2/mnm$ tetragonal lattice, the lattice dimensions *a*, *b* ($a = b$), *c* are given. For the cubic lattice, $a = b = c$. [h] Measured on cooling from isotropic phase. [i] Sphere diameter calculated for $Pm\bar{3}n$ phase using $D = 2(3a^3/32\pi)^{1/3}$ and for the $P4_2/mnm$ phase using $D = 2(abc/40\pi)^{1/3}$. [j] Average column strata thickness calculated from the oriented fiber XRD patterns. [k] Number of dendrimers per supramolecular sphere or per column strata calculated for the *p*6*mm* hexagonal lattice using $\mu = (\sqrt{3}/2)N_A\rho a^2 t/M_{wt}$, for the $Pm\bar{3}n$ phase using $\mu = (1/8)N_A\rho a^3/M_{wt}$, and for the $P4_2/mnm$ phase using $\mu = (1/30)N_A\rho abc/M_{wt}$, where $\rho = 0.96$ (g cm^{-3}) is the experimental density, N_A Avogadro's number, and M_{wt} molecular weight.

Table 3. Wide-Angle Oriented Fiber XRD Data in the Φ_h^{io} Phase for Selected Dendronized Triphenylenes

dendrimer	T (°C)	helix type	c^a (Å)	φ^b (°)	r^c (Å)	$\pi-\pi^d$ (Å)	ξ^e (Å)	ξ/c^f	tilt^g (°)
(3,4)12G1-Tp	24	triple-strand-6_1	4.6	60	8	3.4	27	8	26 ± 5
(3,4Pr)12G1-Tp	25	triple-strand-6_1	4.5	60	9	3.4	37	11	21 ± 5
(3,4,5Pr)12G1-Tp	25	triple-strand-6_1	4.5	60	8.5	–	–	–	21 ± 5
(4)12G0-Tp + TNF (1:1)	26	–	–	–	–	3.4	100	30	46 ± 5

[a] Helical parameter *c* corresponding to layer translation along the column axis. [b] Helical parameter φ corresponding to the layer rotation around the column axis. [c] Average helix radius calculated from the position of the first helical layer line maxima. [d] XRD fiber pattern features assigned to aromatic $\pi-\pi$ stacking interactions. [e] Correlation length of the $\pi-\pi$ stacking features calculated from the full-width at half-maximum. [f] Estimated correlation length of the stacking features converted into numbers of column strata. [g] Dendron tilt angle.

assemble in a helical pyramidal column. The fiber XRD patterns of **(4-3,4,5)12G1-Tp** assemblies show the existence of a weak peak with a *d*-spacing of 3.6 Å, corresponding to the correlation of the average positions of the molecular planes along the column axis. The features of the π-stack peak are very similar to those observed in the case of discotic columnar liquid crystals[1,3,5] and of other columnar assemblies.[6] Similar features indicative of the molecular tilt and short-range helical order, including the presence of the π-stack peak with *d*-spacing of 3.6−3.7 Å with varying degrees of enhancement (Table ST1, Supporting Information), were seen in the oriented fiber XRD patterns of **(4-3,4)12G1-Tp**,**(3,4)12G1-Tp** and **(4)12G0-Tp** in the Φ_h^{io} phase. These molecules show that a π-stack peak with *d*-spacing of 3.6 Å may be suitable to mediate high charge carrier mobility along the column axis, as in the case of other columnar assemblies.[5] Only a few of the oriented fiber XRD patterns collected in the Φ_h^{io} phase show a sufficient number of helical features to be quantitatively analyzed by a combination

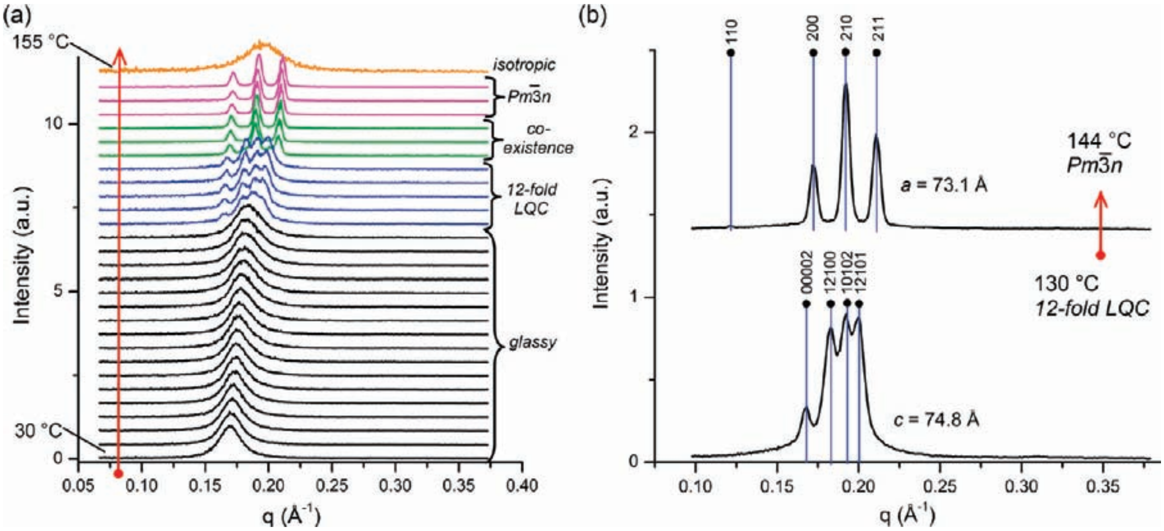

Figure 3. Small-angle XRD powder plots collected for **(3,4-3,5)12G2-Tp** in the 12-fold LQC and $Pm\bar{3}n$ cubic lattices at the indicated temperatures (a) and detailed plots together with indexing at select temperatures (b).

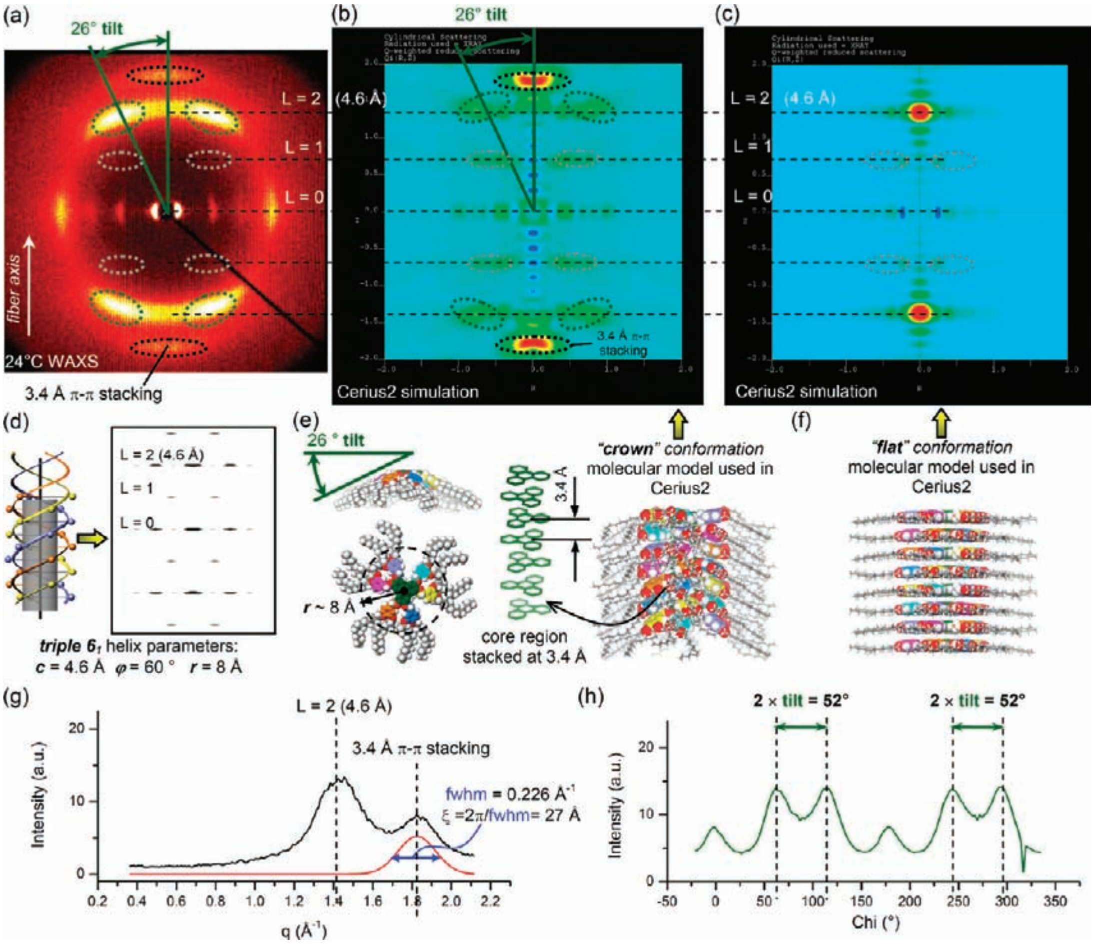

Figure 4. Wide-angle XRD pattern collected from the oriented sample of **(3,4)12G1-Tp** (a). Cerius2 simulations of the XRD fiber pattern (b,c) and the corresponding molecular models (e,f). Identified helical packing and corresponding theoretical fiber pattern (d). Meridional plot indicating the $\pi-\pi$ stacking along the column axis features (g). The correlation length ξ of the $\pi-\pi$ stacking feature is about eight column strata, as calculated from the full width at half-maxima (fwhm). Azimuthal plots integrating the region of the dendron tilt features (h). In panels a−d, helical layer lines (L) are indicated.

of helical diffraction theory applied to simplified atomic helical models[7,14] and by Cerius2 simulations[7] based on their complete supramolecular helical structures.

Determination of the Crown Conformation of (3,4)12G1-Tp, (3,4Pr)12G1-Tp, and (3,4,5Pr)12G1-Tp by the Fiber XRD Patterns. The wide-angle XRD patterns of the oriented fibers of **(3,4)12G1-Tp**, **(3,4Pr)12G1-Tp**, and **(3,4,5Pr)12G1-Tp** were simulated by the helical diffraction theory[7,14] applied to the helical atomic models and by the Cerius2[7] applied to the complete molecular models of the helical pyramidal

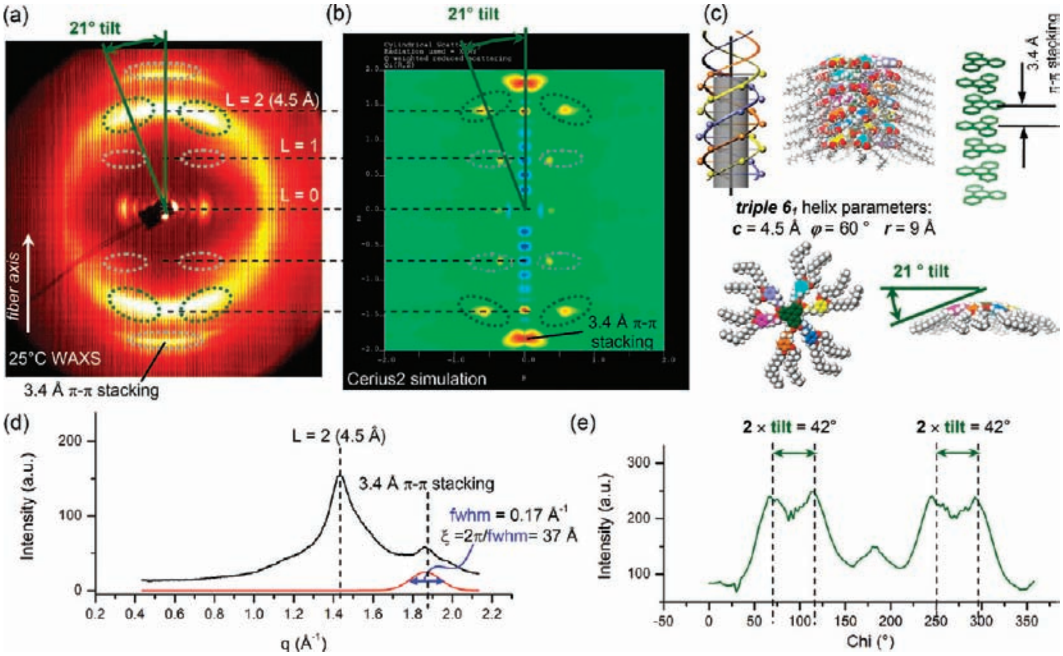

Figure 5. Wide-angle XRD pattern collected from the oriented sample **(3,4Pr)12G1-Tp** (a). Cerius2 simulation of the fiber pattern (b) and the corresponding molecular model (c). Meridional plot indicating the $\pi-\pi$ stacking along the column axis features (d). The correlation length ξ of the $\pi-\pi$ stacking feature is about 11 column strata, as calculated from the full width at half-maxima (fwhm). Azimuthal plots integrating the region of the dendron tilt features (e). In panel a, helical layer lines (L) are indicated, and in panel c, the atomic helix model, identified helix type, and parameters are shown.

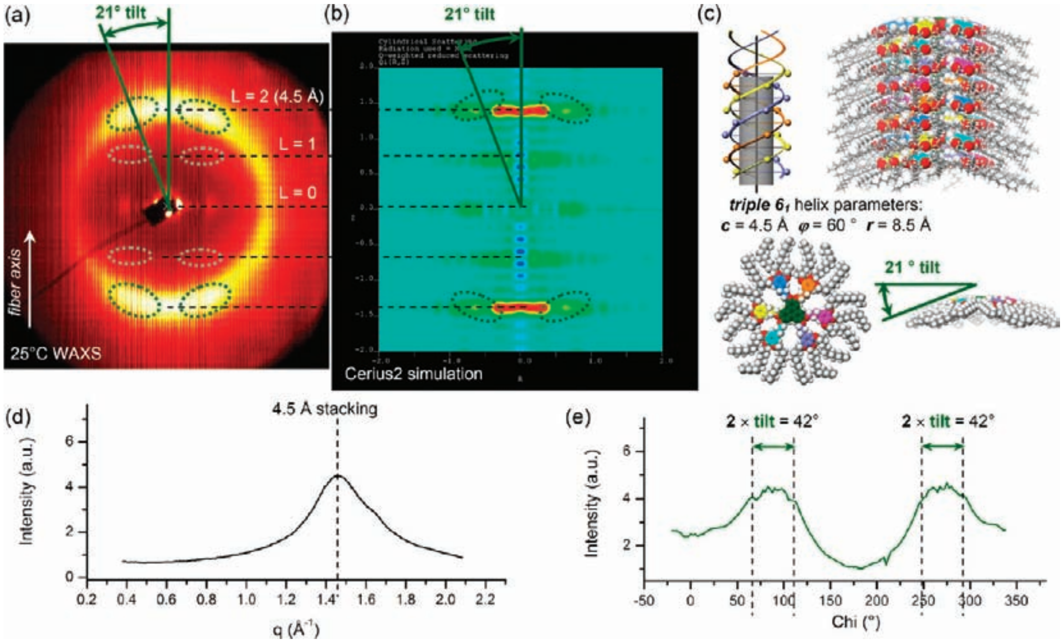

Figure 6. Wide-angle XRD pattern collected from the oriented sample **(3,4,5Pr)12G1-Tp** (a). Cerius2 simulation of the fiber pattern (b) and the corresponding molecular model (c). Meridional plot indicating the stacking along the column axis features (d). Azimuthal plot integrating the region of the dendron tilt features (e). In panels a and b, helical layer lines (L) are indicated, and in panel c, the atomic helix model, identified helix type, and parameters are shown.

columns. The high degree of fiber orientation is demonstrated in Figure SF1 (Supporting Information). Figure 4a shows the wide-angle XRD pattern of the oriented fiber of **(3,4)12G1-Tp**. Analysis of the XRD pattern by helical diffraction theory[14] demonstrated that **(3,4)12G1-Tp** self-assemble in a triple-6_1 atomic helix with the helix parameters and simulated XRD diffractogram shown in Figure 4d. Helical diffraction theory applied to simplified atomic models does not take into account the tilt angle of the pyramidal column and the 3.4 Å $\pi-\pi$ stacking of the Tp units. The assignment of the dendron tilt angle and helical features, and the simulation of the $\pi-\pi$ stacking of Tp units, were possible by Cerius2 simulations of the pyramidal helical column generated from **(3,4)12G1-Tp** dendritic crowns (Figure 4b) and of the helical column made from the disc-like conformation of the same dendronized Tp (Figure 4c). This strategy was presented in a previous publication.[9] The comparison of parts b and c of Figure 4 with part a demonstrates that only the helical

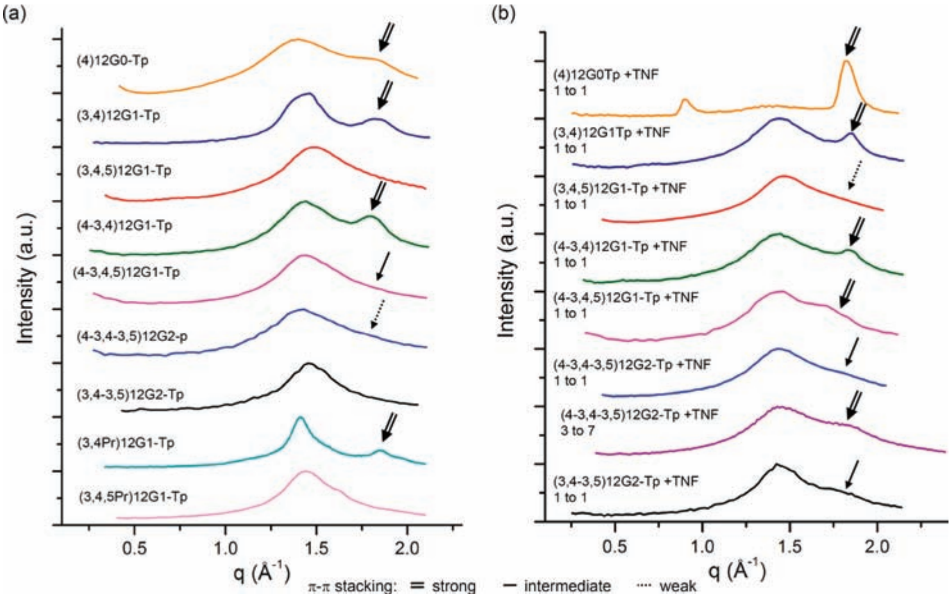

Figure 7. Oriented fiber X-ray diffraction meridional plots collected at 25 °C from the dendronized triphenylenes (a) and from the corresponding dendronized triphenylene−TNF complexes (1:1, 3:7) (b). The $\pi-\pi$ stacking features and their relative intensities are marked.

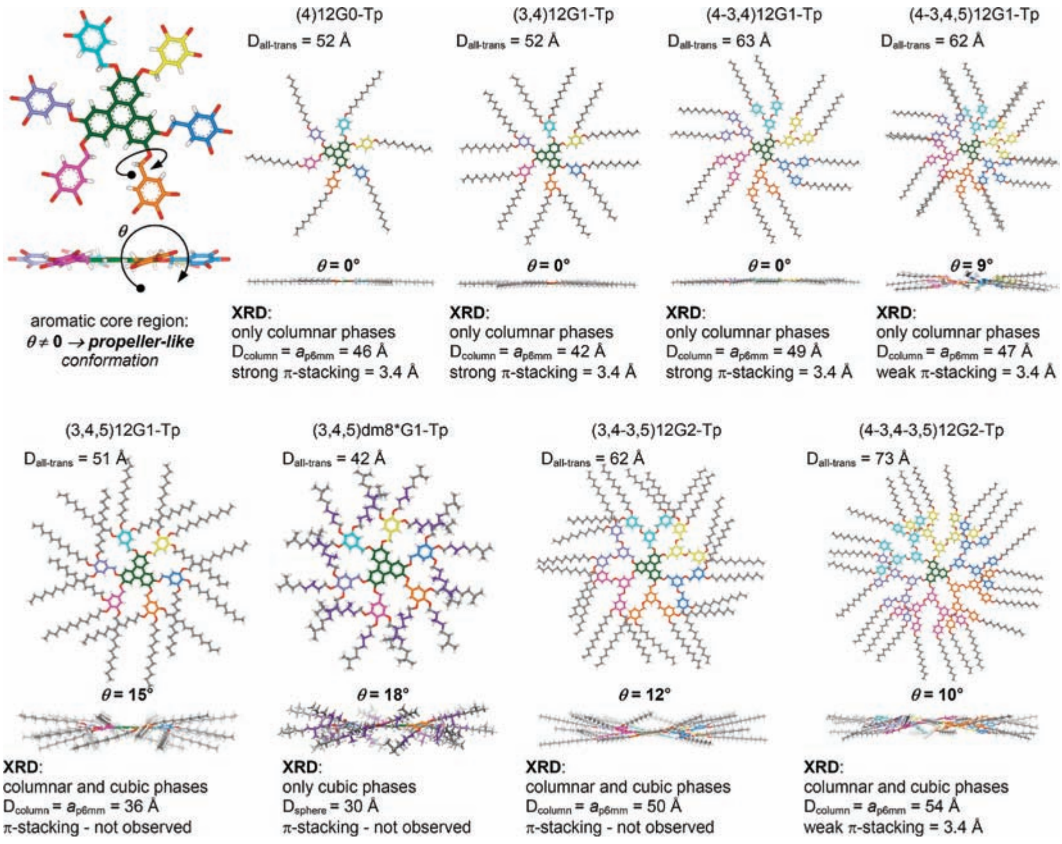

Figure 8. Molecular models of the dendronized triphenylenes in the idealized nonassembled state. In all cases, the aliphatic chains are in an *all-trans* conformation, and the angle θ measures the minimum torsion angle needed to accommodate the steric constraints created by the wider dendrons. Direct correlations between phases and π-stacking features observed in the XRD experiments and the minimum value of the torsion angle θ are indicated.

pyramidal model generated from the crown conformation of **(3,4)12G1-Tp** shown in Figure 4e simulates with a high level of accuracy (Figure 4b) the XRD pattern from Figure 4a. Figure 4g shows the meridional plot of Figure 4a that indicates the 3.4 Å $\pi-\pi$ stacking of the Tp units along the long axis of the helical pyramidal column.

The correlation length ξ of the $\pi-\pi$ stacking feature corresponds to eight Tp units, as calculated from the full width at half-maximum (fwhm): $\xi = 2\pi/\text{fwhm} = 27$ Å (Figure 4g). The azimuthal plot that integrates the region of the dendron tilt features, shown in Figure 4h, provides the dendron tilt angle of 26°. The extent of the helical or stacking correlations is

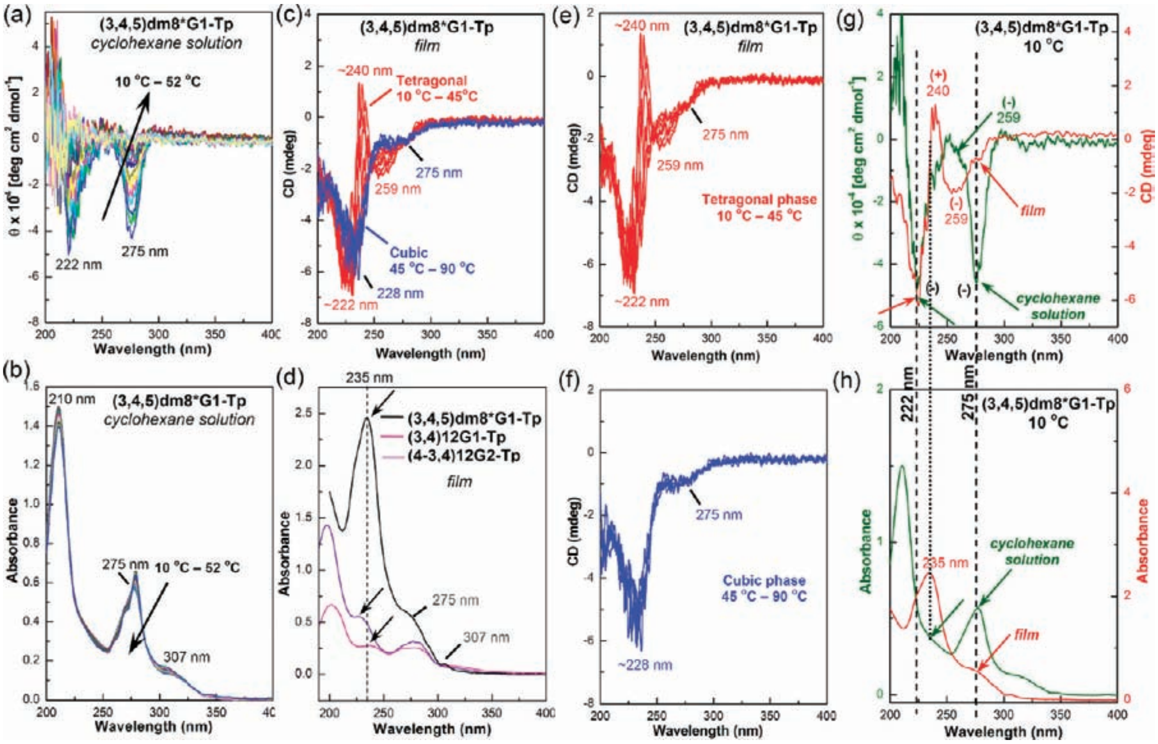

Figure 9. Temperature dependence of the CD and UV spectra of **(3,4,5)dm8*G1-Tp** in cyclohexane solution (7.8×10^{-5} M) (a,b) and CD spectra in spin-coated film cast from $CHCl_3$ (10%, w/v) (c). Combined UV spectra of **(3,4,5)dm8*G1-Tp**, **(3,4)12G1-Tp**, and **(4-3,4)12G2-Tp** in spin-coated film cast from $CHCl_3$ (d). Temperature-dependent CD spectra of **(3,4,5)dm8*G1-Tp** in the tetragonal phase, in the temperature range 10−45 °C (c), and in the cubic phase, in the temperature range 45−90 °C (g). Overlay of the CD and UV spectra at 10 °C in both cyclohexane solution (7.8×10^{-5} M) and spin-coated film cast from $CHCl_3$ (10%, w/v) (d,h).

concurrently limited by the difference in the values of the core stacking of 3.4 Å and of the helical parameter c of 4.5 Å. In other words, the mismatch of the Tp core tight packing with the outer helical packing of the dendritic shell explains why the helical and $\pi-\pi$ correlations are limited to an average of eight column strata (Figure 4g).

A similar series of simulations was used for the analysis of the helical pyramidal columns assembled from **(3,4Pr)12G1-Tp** (Figure 5) and **(3,4,5Pr)12G1-Tp** (Figure 6). The replacement of the (3,4)12G1-benzyl ether dendron (Figure 4) with the (3,4Pr)12G1-propyl ether dendron (Figure 5) mediates a longer correlation length of the $\pi-\pi$ stacking of the Tp units (Figures 5a and 6a) and decreases the tilt angle of the dendritic crown (Figures 4e and 5c). Both results are expected, considering that the longer Tp−dendron propyl linkage relaxes some of the packing constrains observed in the **(3,4)12G1-Tp** (Figure 4). The triple-6_1 atomic helix model was not affected by this structural change. When the **(3,4Pr)12G1** dendron was replaced with **(3,4,5Pr)12G1** dendron, the tilt angle of the **(3,4,5Pr)12G1-Tp** did not change. However, the $\pi-\pi$ stacking of the Tp units is not observed in the XRD patterns from Figure 6a. The change from benzyl ether to propyl ether and its consequences on the $\pi-\pi$ stacking of the Tp units in the pyramidal column indicate pathways to program the arrangement of the electroactive organic elements at the molecular level.

The relationship between the structure of the dendron and the $\pi-\pi$ stacking of the Tp is illustrated by the XRD plots from Figure 7a. The general trend is that "sharp" dendrons exhibit strong $\pi-\pi$ stacking correlations, whereas for "wide" dendrons these correlations are weak or absent. Figure 8 demonstrates the correlation of the dendritic architecture with the self-assembly mechanism of the dendronized triphenylenes. These models represent the ideal conformation in the nonassembled state. The torsion angle θ, defined in Figure 8, is used to demonstrate the correlation of the dendron solid angle with the intensity of the π-stacking features and with the presence of cubic or tetragonal phases upon self-assembly. Dendrons with small solid angle,[6a] such as **(4)12G0**, **(3,4)12G1**, **(4-3,4)12G1**, and **(4-3,4,5)12G1**, can accommodate the packing constraints of the hexa-substituted Tp core without any torsion ($\theta = 0$, Figure 8). On the other hand, dendrons with large solid angle, such as **(3,4,5)12G1**, **(3,4-3,5)12G2**, and **(4-3,4-3,5)12G2**, require an increase of the θ torsion angle proportional to their solid angle. Therefore, Tp functionalized with dendrons with large solid angle have an increased probability of forming cubic or tetragonal phases upon self-assembly, and at the same time, they disfavor long-range core π-stacking interactions. Based on this idealized nonassembled state representation, the self-assembly of dendronized triphenylenes is well mapped as a function of the dendritic architecture from Figure 8. Furthermore, it is clear why the addition of the chiral center to the aliphatic region of the **(3,4,5)G1** dendron suppressed the formation of any columnar phase upon the self-assembly of **(3,4,5)dm8*G1-Tp**. In this case, the minimum torsion angle θ, required to accommodate the hexa-substituted Tp core packing constraints, has the largest value.

The results observed suggest that the spherical supramolecular dendrimers assembled from the dendronized Tp are constructed from short fragments of helical pyramidal columns that are spherically distorted. XRD experiments performed on oriented fibers provide the definitive molecular structure and the internal order of the helical pyramidal columns. However, due to the

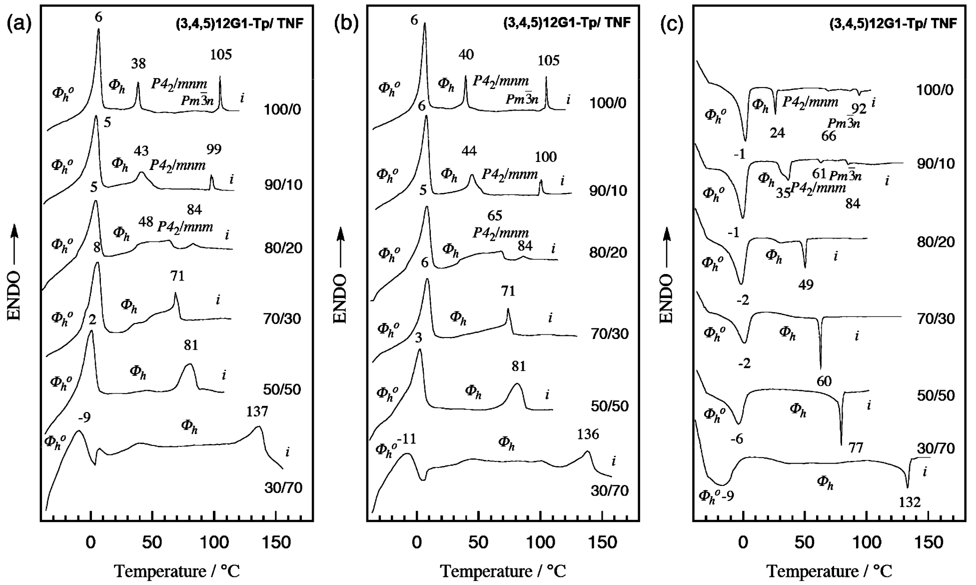

Figure 10. DSC traces (5 °C/min) of donor−acceptor complexes of **(3,4,5)12G1-Tp** with **TNF** at different molar ratios: (a) first heating, (b) second heating, and (c) first cooling scans. The phase transitions and transition temperatures are indicated.

isotropic nature of the cubic lattice, XRD experiments on fibers generated from lattices assembled from spherical dendrimers do not provide additional structural information on the intramolecular structure of the supramolecular spheres. The only additional information that can be obtained is available from circular dichroism (CD) experiments carried out on spherical supramolecular assemblies containing stereocenters in their alkyl groups (Scheme 1) or by complexation of the Tp part of the dendritic crown with a chiral acceptor.

Analysis of Chiral Supramolecular Spheres Assembled from Chiral Dendritic Crowns by CD Experiments. Incorporation of a branched stereocenter in the alkyl groups of **(3,4,5)12G1-Tp** generated **(3,4,5)dm8*G1-Tp** (Scheme 1). The presence of stereocenters in the alkyl chains favors self-assembly into the spherical supramolecular dendrimers that self-organize in cubic and tetragonal lattices. The Φ_h phase exhibited by the nonchiral molecule at low temperatures was eliminated (Tables 1 and 2). This facilitated the self-assembly of spherical supramolecular dendrimers that self-organize in tetragonal and cubic lattices, which are stable from room temperature up to 84.5 °C (Table 1). This wider thermal stability range facilitated analysis by CD experiments carried out both in solvophobic solvents and in film (Figure 9). The CD spectrum obtained in cyclohexane solution shows that the spherical supramolecular dendrimers are chiral between 10 and 52 °C (Figure 9a). The UV spectrum of **(3,4,5)dm8*G1-Tp** shows five isosbestic points at 222, 257, 267, 275, and 324 nm that demonstrate an equilibrium between the individual dendronized Tp and their supramolecular assembly (Figure 9b). Above 52 °C, **(3,4,5)dm8*G1-Tp** exists as a molecular solution. Therefore, the assembly of the dendronized Tp crown into the chiral supramolecular sphere, observed as the transfer of the chirality from the alkyl groups of **(3,4,5)dm8*G1-Tp** to its aromatic region (Figure 9a), demonstrates that the structure of the supramolecular sphere must be equipped with a mechanism that amplifies the molecular chirality. This amplification is provided by the short helical pyramidal column from the inner part of the sphere. The CD in film was recorded between 10 and 90 °C (Figure 9c). The spheres self-organize in a tetragonal lattice in the temperature range of 10−40 °C, while between 45 and 85 °C the supramolecular spheres self-organize in a cubic lattice (Table 1). The CD experiments in film demonstrate that the supramolecular spheres are chiral in both tetragonal (Figure 9c,e) and cubic lattices (Figure 9c,f). If we compare parts e and f of Figure 9, we observed that there is a small difference between the CD of the supramolecular spheres in these two lattices. In the cubic lattice four spheres are distorted in tetragonal shapes,[10a] while in the tetragonal lattice eight spheres[10b] are distorted.[10,15] Therefore, in the tetragonal lattice more spheres have columnar character than in the cubic lattice.[15] The supramolecular spheres generated in dilute solution (Figure 9a), most probably, are not distorted. This structural difference is most probably responsible for the difference between the CD spectra shown in Figure 9e,f. The CD spectrum was also recorded in the isotropic state at 90 °C. Even at this temperature, the supramolecular spheres exist and are chiral.

The UV/CD spectra of the spin-coated film in the tetragonal but not in the cubic phase indicate a potential exciton coupling positioned at the 235 nm maximum in the UV absorption (Figure 9 g,h). The two Cotton effects observed in the film CD spectrum of the tetragonal phase, negative at 222 nm and positive at 240 nm (Figure 9g), with the zero crossing at 235 nm, seem to indicate a positive exciton coupling for the **(3,4,5)dm8*-Tp** functionalized with (*S*) chiral centers in the alkyl group from the dendron periphery.

These experiments demonstrate that the supramolecular spheres are chiral and that they are equipped with a mechanism that amplifies chirality. The amplification of chirality is generated by the short fragments of helical pyramidal columns that are spherically distorted and generate the inner part of the sphere. These results are in agreement with those obtained when conformationally rigid dendritic crowns were used to self-assemble chiral supramolecular spheres.[9a] A comparison of the CD spectra obtained from

---

(14) (a) Cochran, W.; Crick, F. H. C.; Vand, V. *Acta Crystallogr.* **1952**, *5*, 581–586. (b) Klug, A.; Crick, F. H. C.; Wyckoff, H. W. *Acta Crystallogr.* **1958**, *11*, 199–213.

(15) Dukeson, D. R.; Ungar, G.; Balagurusamy, V. S. K.; Percec, V.; Johansson, G. A.; Glodde, M. *J. Am. Chem. Soc.* **2003**, *125*, 15974–15980.

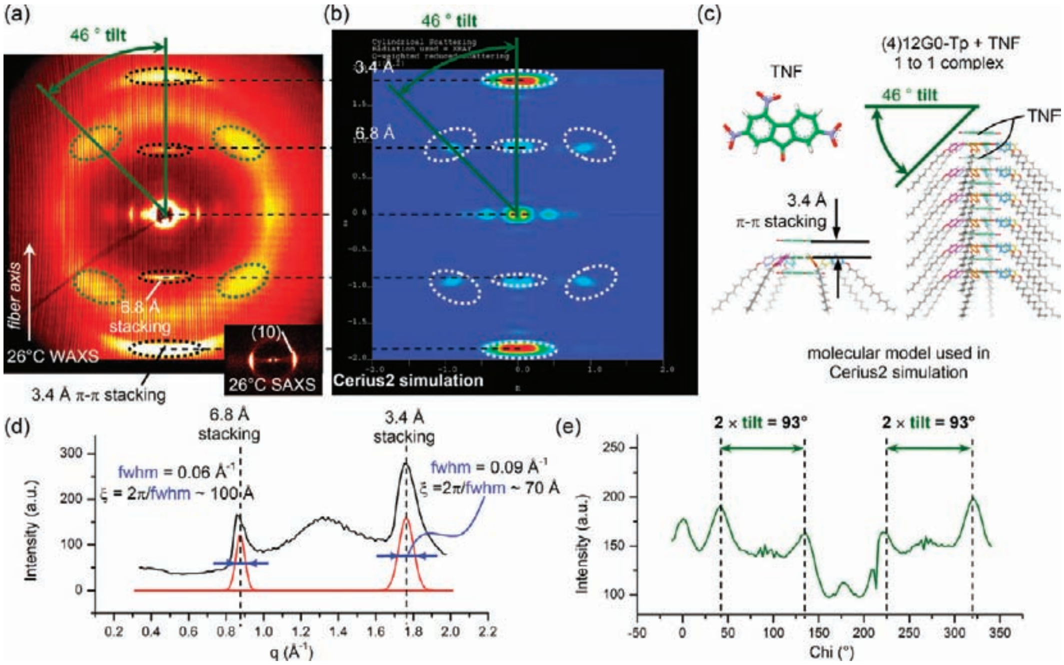

Figure 11. The 1/1 donor−acceptor complex of **(4)12G0-Tp** with TNF enhances the aromatic $\pi-\pi$ stacking interactions and induces a crown conformation of the dendronized Tp. Wide-angle oriented fiber pattern collected at 25 °C from the complex (a) and Cerius2 simulation of the molecular model of the crown conformation in the pyramidal column (b). Molecular model of the dendronized Tp used in the Cerius2 simulation (c). Meridional plots of the fiber pattern from panel a, indicating the two stacking along the column features; the correlation length ξ of the stacking features is about 30 column strata (d). Azimuthal angle chi plots integrating the area along the wide-angle features corresponding to dendron tilt correlations (e). In panels a, b, c, and e, the dendron tilt features and the agreement between experimental and simulated tilt angle are indicated.

(3,4,5)dm8*G1-Tp in cyclohexane solution at 10 °C and in the tetragonal phase at 10 °C is shown in Figure 9g. The negative Cotton effects at 222, 259, and 275 nm are observed in both solution and film, although their ellipticity differs in the two states. Nevertheless, they exhibit sufficient similarity to consider that the assemblies in film and solution are generated from similar crown conformations. Furthermore, the potential positive exciton coupling observed in film is associated with an increase of the UV absorption shoulder from solution at 235 nm to an absorption maximum in film state (Figure 9d). Similar absorption maxima at 235 nm were observed in the UV spectra of **(3,4)12G1-Tp** and **(4-3,4)12G2-Tp** in spin-coated films (Figure 9d). This indicates that the absorption maximum at 235 nm of **(3,4,5)dm8*G1-Tp** in film (Figure 9d) does not represent a bathochromic shift of the UV maximum observed in solution at 210 nm (Figure 9b). The peak at lower wavelength is also available in film, but its absorption is too high to be shown in Figure 9d.

Programming the Self-Assembly Process via Donor−Acceptor Interactions. Disc-like triphenylenes interact with electron-acceptor compounds both in solution and in bulk self-assembled state.[16] Reversible interactions along the supramolecular column act as a supramolecular “polymer backbone”.[17] It has also been demonstrated that a covalent backbone with increasing degrees of polymerization can change the self-assembly of a dendronized polymer containing conical dendritic side groups from supramolecular spheres to supramolecular columns.[18] Previously, donor−acceptor interactions were used to generate reversible networks from linear polymer backbones containing donor and acceptor side groups,[19] and to create supramolecular dendronized polymers.[19c] Therefore, it is interesting to address the following new challenge. Would a supramolecular polymer backbone created via donor−acceptor interactions be able to program the self-assembly of dendritic crowns created from the donor Tp? Figure 10 provides the first answer to this question. **(3,4,5)12G1-Tp** (Scheme 1) was selected for this experiment since it self-assembles into helical pyramidal columns that self-organize in Φ_h phase and in supramolecular spheres that self-organize in tetragonal and cubic lattices. It was also demonstrated in the previous subsection that these columns and spheres are chiral, and therefore, the incorporation of a stereocenter in various parts of the dendronized Tp, such as shown in Figure 9 for the alkyl part of the dendron, is expected to select the helical sense of the supramolecular object. In these series of experiments, it will be

---

(16) (a) Green, M. M.; Ringsdorf, H.; Wagner, J.; Wüstefeld, R. *Angew. Chem., Int. Ed. Engl.* **1990**, *29*, 1478–1481. (b) Gallivan, J. P.; Schuster, G. B. *J. Org. Chem.* **1995**, *60*, 2423–2429.

(17) For examples of supramolecular polymers mediated by non-covalent interactions see: (a) Percec, V.; Johansson, G.; Heck, J.; Ungar, G.; Batty, S. V. *J. Chem. Soc., Perkin Trans. 1* **1993**, 1411–1420. (b) Percec, V.; Johansson, G.; Ungar, G.; Zhou, J. *J. Am. Chem. Soc.* **1996**, *118*, 9855–9866. (c) Percec, V.; Holerca, M. N.; Uchida, S.; Cho, W.-D.; Ungar, G.; Lee, Y.; Yeardley, D. J. P. *Chem.-Eur. J.* **2002**, *8*, 1106–1117. (d) Percec, V.; Cho, W.-D.; Ungar, G.; Yeardley, D. J. P. *Chem.-Eur. J.* **2002**, *8*, 2011–2025. (e) Ungar, G.; Abramic, D.; Percec, V.; Heck, J. A. *Liq. Cryst.* **1996**, *21*, 73–86. (f) Percec, V.; Bera, T. K.; Glodde, M.; Fu, Q.; Balagurusamy, V. S. K.; Heiney, P. A. *Chem.-Eur. J.* **2003**, *9*, 921–935.

(18) (a) Percec, V.; Ahn, C. H.; Ungar, G.; Yeardley, D. J. P.; Möller, M.; Sheiko, S. S. *Nature (London)* **1998**, *391*, 161–164. (b) Percec, V.; Holerca, M. N. *Biomacromolecules* **2000**, *1*, 6–16. (c) Percec, V.; Holerca, M. N.; Uchida, S.; Yeardley, D. J. P.; Ungar, G. *Biomacromolecules* **2001**, *2*, 729–740.

(19) (a) Rodriguez-Parada, J. M.; Percec, V. *Macromolecules* **1986**, *19*, 55–64. (b) Pugh, C.; Percec, V. *Macromolecules* **1986**, *19*, 65–71. (c) Percec, V.; Glodde, M.; Bera, T. K.; Miura, Y.; Shiyanovskaya, I.; Singer, K. D.; Balagurusamy, V. S. K.; Heiney, P. A.; Schnell, I.; Rapp, A.; Spiess, H.-W.; Hudson, S. D.; Duan, H. *Nature (London)* **2002**, *419*, 384–387.

Scheme 2. Synthesis of D- and L-Menthol−TNF

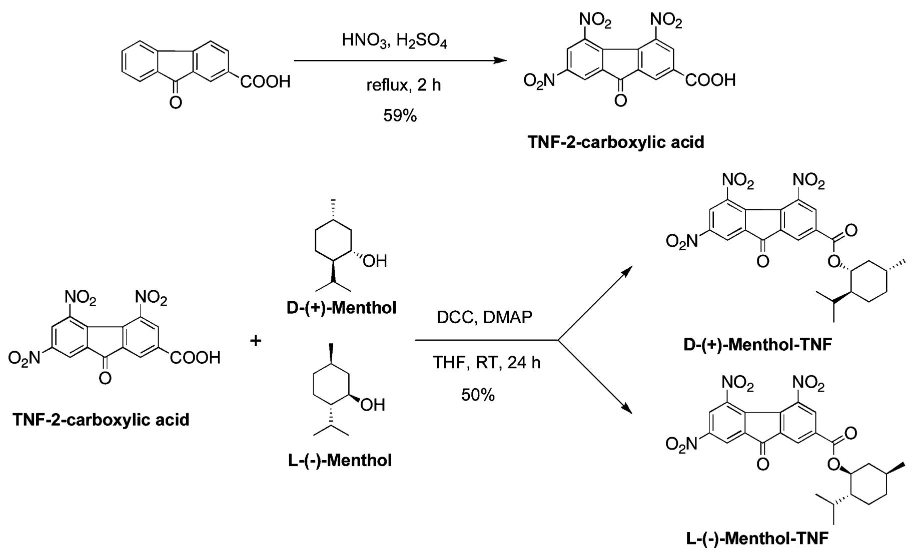

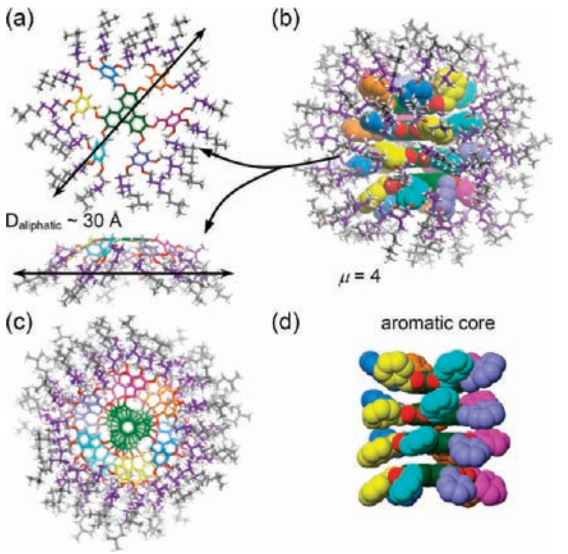

Figure 12. Molecular model of the supramolecular chiral spherical dendrimers self-assembled from **(3,4,5)dm8*G1-Tp**. Top and side views of the crown-like conformation of the dendronized Tp (a). Side (b) and top (c) views of the chiral spherical supramolecular dendrimer generated from a spherically distorted helical pyramidal column. Detail of the helical pyramidal packing of the aromatic core region (d).

demonstrated that the stereocenter can be located also on the alkyl part of the acceptor.

The heating and cooling DSC traces of **(3,4,5)12G1-Tp** and its complex with 2,4,7-trinitrofluorenone (TNF) with various molar ratios are shown in Figure 10. The data in Figure 10 demonstrate a very clear trend. The donor−acceptor complex between the Tp part of the dendritic crown and TNF enhances the thermal stability of the helical pyramidal column that self-organizes in the Φ_h phase. At the same time, it decreases the thermal stability of the tetragonal and cubic lattices self-organized from supramolecular spheres. Therefore, while the temperature of the transition from Φ_h to tetragonal lattice increases, the temperature of the transition from cubic to isotropic liquid decreases. As the concentration of electron-donor−acceptor complex (EDA) increases, the cubic phase disappears, the temperature of the transition from Φ_h to tetragonal increases, and the isotropization transition changes from cubic→isotropic to tetragonal→isotropic. As a result, the temperature range of the tetragonal phase decreases and ultimately the tetragonal phase disappears. Above 30 mol % TNF the only supramolecular structure observed is the helical pyramidal column. At 70 mol % TNF the original transition from Φ_h to tetragonal from 40 °C transfers into Φ_h to isotropic and moves to 136 °C. This trend is identical to that generated by an increased degree of polymerization of a covalent polymer[18] and corresponds to a supramolecular polymer effect[17,20,21] that can be explained via thermodynamic schemes that correlate various ordered states.[20] The supramolecular polymer effect mediated by EDA interactions also supports the spherically distorted short helical pyramidal column mechanism for the formation of the chiral supramolecular spheres. An increased strength of the interaction in the column is similar to a longer covalent polymer backbone[18] and, therefore, disfavors the formation of supramolecular spheres and favors the formation of helical pyramidal columns. This supramolecular "polymer effect" is also supported by XRD experiments. Figure 11a shows the XRD obtained from the aligned fiber of **(4)12G0-Tp** with TNF. The Cerius2 simulation and the crown conformation of the dendritic Tp−TNF complex are shown in Figure 11b,c. The (4)12G0-Tp uncomplexed structure does not show any tilt features (compare Figure SF1 with Figure 11a−d). Complexation with TNF induces both a crown conformation and a stronger π-stacking. The correlation length of the π-stacking EDA interactions spans more than 30 column strata. This value is approximately 4 times the correlation length of the non-complex-dendronized triphenylenes, confirming the formation of a donor−acceptor complex between the Tp

---

(20) Percec, V.; Keller, A. *Macromolecules* **1990**, *23*, 4347–4350.

(21) (a) Brunsveld, L.; Folmer, B. J. B.; Meijer, E. W.; Sijbesma, R. P. *Chem. Rev.* **2001**, *101*, 4071–4098. (b) Sijbesma, R. P.; Meijer, E. W. *Curr. Opin. Colloid Interface Sci.* **1999**, *4*, 24–32. (c) Moore, J. S. *Curr. Opin. Colloid Interface Sci.* **1999**, *4*, 108–116. (d) Moore, J. S. *Curr. Opin. Colloid Interface Sci.* **1999**, *4*, 108–116. (e) Emrick, T.; Fréchet, J. M. J. *Curr. Opin. Colloid Interface Sci.* **1999**, *4*, 15–23. (f) Sherrington, D. C.; Taskinen, K. A. *Chem. Soc. Rev.* **2001**, *30*, 83–93. (g) Keizer, H. M.; Sijbesma, R. P. *Chem. Soc. Rev.* **2005**, *34*, 226–234. (h) Lehn, J. M. *Makromol. Chem. Macromol. Symp.* **1993**, *69*, 1–17. (i) Lehn, J. M *Polym. Int.* **2002**, *51*, 825–839. (j) Berl, V.; Schmutz, M.; Krische, M. J.; Khoury, R. G.; Lehn, J. M. *Chem.-Eur. J.* **2002**, *8*, 1227–1244. (k) Rudick, J. G.; Percec, V. *Acc. Chem. Res.* **2008**, 1641–1652.

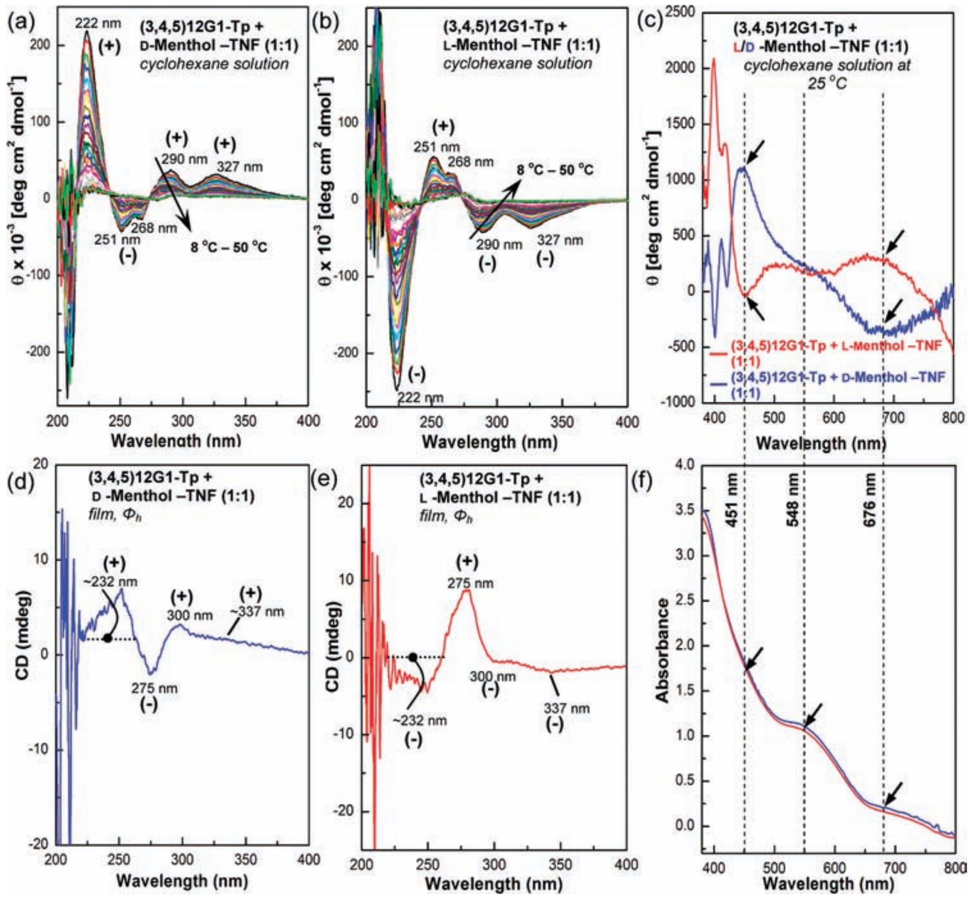

Figure 13. Temperature dependence of the CD spectra of 1:1 donor−acceptor complexes of **(3,4,5)12G1-Tp** + D-menthol−TNF (a) and **(3,4,5)12G1-Tp** + L-menthol−TNF (b) in cyclohexane solution (1.1 × 10^{-4}M). The CD and UV spectra of 1:1 donor−acceptor complexes of **(3,4,5)12G1-Tp** and D-(+)- and L-(−)-menthol−TNF (1:1) in cyclohexane solution (1.3 × 10^{-2}M) at 25 °C (c,f); **(3,4,5)12G1-Tp** + D-menthol−TNF (1:1) in spin-coated film cast from $CHCl_3$ (1.8%) at 10 °C (d); and **(3,4,5)12G1-Tp** + L-menthol−TNF (1:1) in spin-coated film cast from $CHCl_3$ (1.8%) at 10 °C (e).

aromatic core and the TNF. As consequence, complexation experiments together with XRD and CD results support the mechanism of assembly in chiral supramolecular spheres that is outlined in Figure 12.

Selecting the Sense of a Helical Pyramidal Column via EDA Complexes with Chiral Acceptors. The synthesis of the esters of D-(−)-menthol and L-(−)-menthol with 4,5,7-trinitro-9-oxo-9*H*-fluorene-2-carboxylic acid (D-menthol−TNF and L-menthol−-TNF) is outlined in Schemes 2 and SS3 (Supporting Information). The 1:1 EDA complexes of L-menthol−TNF and D-menthol−TNF with **(3,4,5)12G1-Tp** eliminate the tetragonal and cubic phases of the parent dendronized Tp, and therefore, the donor−acceptor complex self-assembles only into helical pyramidal columns. This complex was investigated by CD experiments carried out in cyclohexane solution and in film. The CD experiments performed in film showed the absence of linear dichroism (Supporting Information, Figure SF9). Figure 13a,b shows the CD spectra as a function of temperature for the complex with D- and L-menthol−TNF. These two sets of CD spectra are mirror images. They demonstrate the assembly of left- and right-handed helical pyramidal columns. The sense of these columns was selected by the D- and L-stereocenters of the acceptor via the donor−acceptor interaction with the Tp part of the dendronized Tp. With increasing the temperature from 8 to 50 °C, the elipticity of all Cotton effects decreases. At 50 °C, no Cotton effect is observed. Each set of CDs shows two isodichroic points that correlate with the isosbestic points from the UV spectra (Supporting Information, Figure SF7). The temperature dependence of these CDs is reversible on repeated heating and cooling scans.

Figure 13c,f shows the CD spectra recorded in solution in the range of the charge-transfer complex shown in the UV−vis spectra from Figure 13f. A much higher concentration was used to record the CD in this area. Nevertheless, the CD spectra from Figure 13c show that the charge-transfer complexes are also mirror images. Since the UV absorption of the films is too high in the 200−250 nm range (Supporting Information, Figure SF7) at lower wavelength, the most relevant part of the film CD spectra is provided by the Cotton effects at 232, 275, 300, and 337 nm (Figure 13d,e). These four Cotton effects show signs identical with those observed in solution (Figure 13a,b) except that in film they are shifted by about 10 nm toward higher wavelengths. In addition, due to lower resolution in film, the elipticities from 251 and 268 nm in solution seem to be merged in film in a single signal at 275 nm. These CD spectra show a dependence on temperature similar to that in solution, and they correlate with the transition temperature observed by DSC (Supporting Information, Figure SF8). Therefore, these experiments seem to indicate related mechanisms of self-assembly in solution and in film.

Analysis of the (3,4,5)12G1-Tp Self-Assembly Process by Solid-State ^{1}H and ^{13}C NMR. The **(3,4,5)12G1-Tp**-dendronized Tp and the corresponding donor−acceptor complexes with TNF were selected for a solid-state NMR study[3e,19c,22] in order to

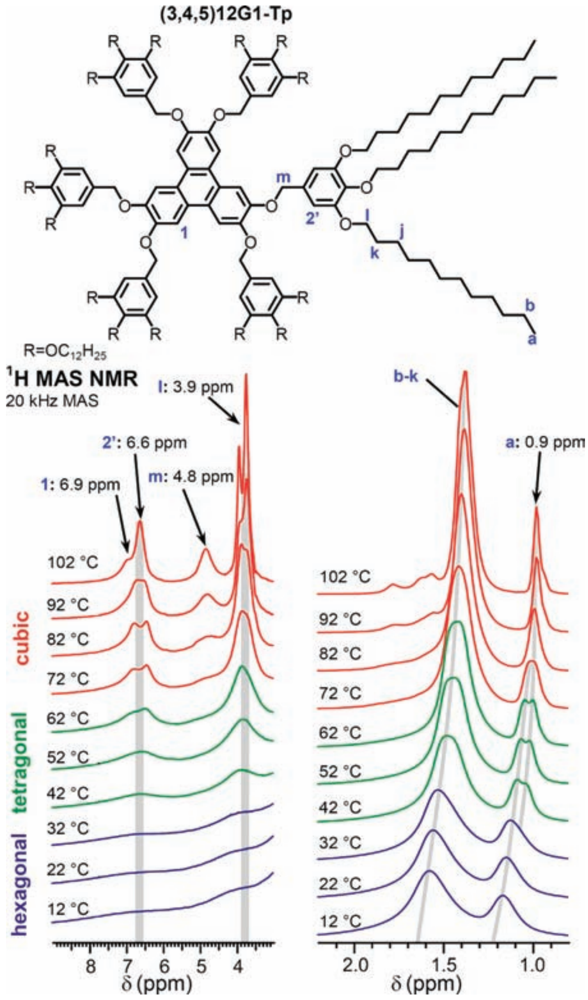

Figure 14. Variable-temperature solid-state ^{1}H MAS NMR spectra of the **(3,4,5)12G1-Tp**-dendronized triphenylenes. Temperatures, phases, and assignments are indicated.

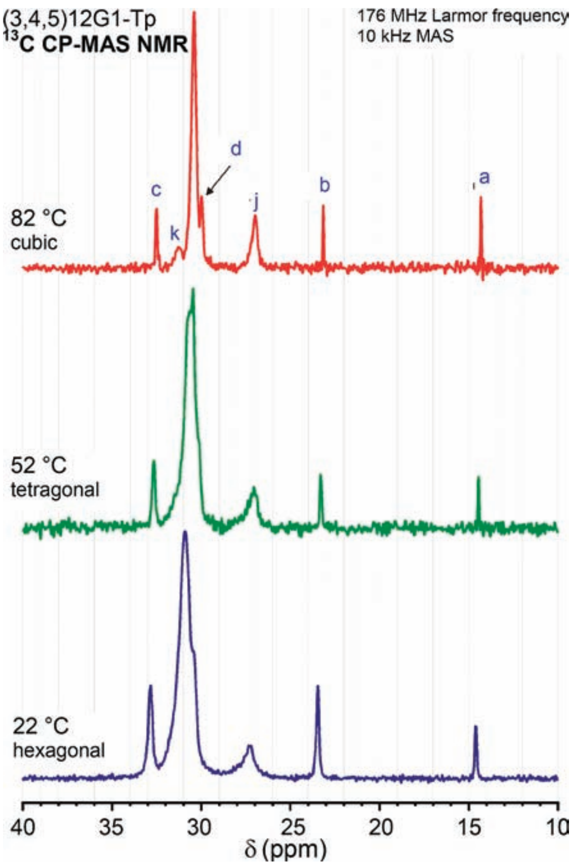

Figure 15. Variable-temperature solid-state ^{13}C CP-MAS NMR spectra of the **(3,4,5)12G1-Tp**-dendronized triphenylenes. Assignments labeled as in Figure 14.

identify structural changes at the transition from columnar hexagonal, to tetragonal, and to cubic phases. Previously, it has been shown that solid-state NMR analysis is complementary to XRD experiments.[19c,22c] In the cubic phase, at 102 °C (Figure 14), close to the isotropization temperature, the ^{1}H MAS NMR spectrum of **(3,4,5)12G1-Tp** is well resolved, and therefore, different protons of the molecule could be assigned. The first important remark is that the ^{1}H signals of the triphenylene core, which are observed at 8.3 ppm in chloroform solution, appear at 6.9 ppm in the solid-state ^{1}H NMR spectrum and are separated by only 0.3 ppm from the protons of the dendritic phenyl rings containing aliphatic side chains. This upfield shift of the Tp core signals results from substantial π-stacking of the triphenylene core and demonstrates π-stacking even when XRD experiments could not detect it (Figure 7). The chemical shifts of the dendritic outer phenyl rings in the cubic phase are very close to those observed in the spectra recorded in solution. The OCH$_2$ group is observed at 4.8 ppm as a broad solid-like peak, whereas the signals of the aliphatic side chains exhibit an almost liquid-like shape. It should be noted that the signal of the outer phenyl OCH$_2$ group from 3.9 to 3.7 ppm is split, with the intensity ratio 1:2 attributed to the para and meta positions of the side chains and their resulting position with respect to the ring current of the phenyl ring.

At lower temperatures, all signals observed in Figure 14 are substantially broadened. This, however, does not result from dipolar broadening often observed in rigid ^{1}H systems but rather from an incomplete averaging of a heterogeneous chemical shift distribution due to the triphenylene core. In the tetragonal phase, however, the π shift for the triphenylene protons can still be resolved and is virtually unchanged. This indicates that the π-stacking in the tetragonal and the cubic phases is essentially the same, apart from some line narrowing due to local molecular fluctuation. The ^{1}H spectra in the hexagonal phase are even less resolved, yet there is no indication of a change of π-stacking. These results support the supramolecular structures advanced by XRD experiments. Remarkably, the CH$_3$ end group exhibits a temperature-dependent shift by more than 0.2 ppm. Moreover, the signal splits upon the transition from hexagonal to tetragonal phase. This splitting vanishes upon transition to the more symmetric cubic phase.

In the case of variable-temperature ^{13}C CP-MAS measurements (Figure 15), the carbon signals of the aliphatic chains exhibit the same temperature-dependent change in chemical shift as observed in the ^{1}H MAS spectra shown in Figure 14. The CP-MAS spectrum recorded at 82 °C, where the last four positions (a−d) as well as the j and k positions of the aliphatic side chains are spectrally resolved, is indicative of a gradient of mobility along the aliphatic chain. The signals from sites close to the chain ends are very narrow due to their conforma-

---

(22) (a) Spiess, H. W. *J. Polym. Sci., Part A: Polym. Chem.* **2004**, *42*, 5031–5044. (b) Brown, S. P.; Spiess, H. W. *Chem. Rev.* **2001**, *101*, 4125–4155. (c) Percec, V.; Glodde, M.; Peterca, M.; Rapp, A.; Schnell, I.; Spiess, H. W.; Bera, T. K.; Miura, Y.; Balagurusamy, V. S. K.; Aqad, E.; Heiney, P. A *Chem.-Eur. J.* **2006**, *12*, 6298–6314.

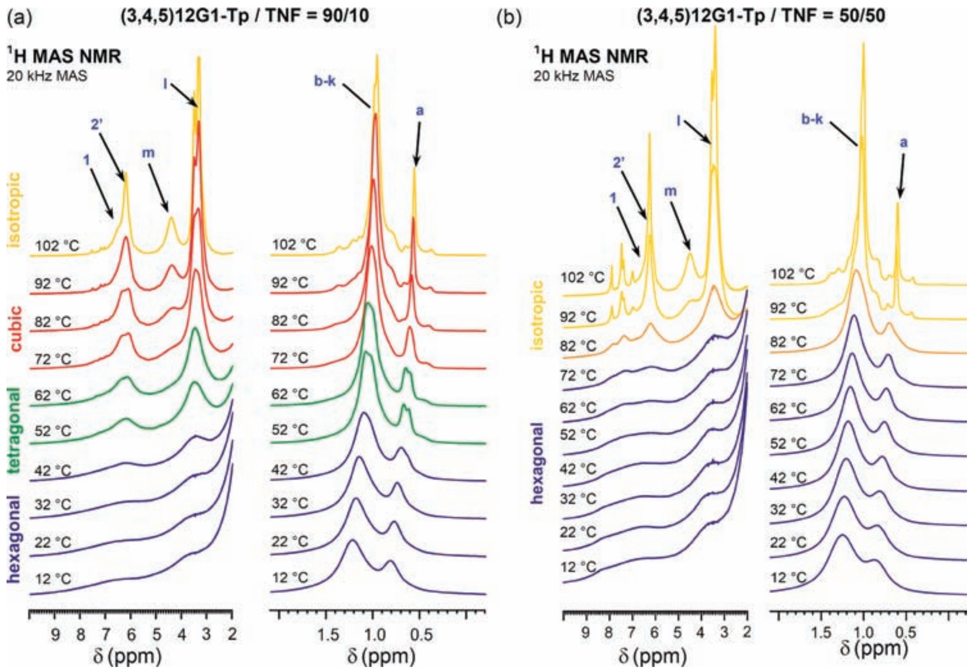

Figure 16. Variable-temperature solid-state ^{1}H MAS NMR spectra of the complex **(3,4,5)12G1-Tp**−TNF = 90/10 (a) and 50/50 (b). Temperatures, phases, and assignments are indicated.

tional exchange in the fast motional limit, whereas sites close to the OCH_2 group are observed with substantial broadening due to slower conformational exchange. The splitting of the alkyl chain end methyl ^{1}H signal in the tetragonal phase is not observed in the ^{13}C NMR spectrum, and thus this splitting is attributed to differences in the local packing of the methyl groups rather than to conformational differences of the aliphatic side chains.

The ^{1}H MAS spectra of two **(3,4,5)12G1-Tp**−TNF donor−acceptor complexes are shown in Figure 16. Besides small shifts, the ^{1}H MAS spectra of the **(3,4,5)12G1-Tp**−TNF 90/10 complex exhibit thermal trends similar to those observed for the pure compound. Above 82 °C, the TNF spectra can be identified in the 7−8 ppm range of the **(3,4,5)12G1-Tp**−TNF 90/10 and 50/50 complexes. This corresponds to an upfield shift of the different TNF signals due to π-stacking by 1.0−1.5 ppm compared to the ^{1}H NMR spectrum of TNF dissolved in chloroform. This shift is comparable to that experienced by the protons of the TP cores. Since the TNF signals are observed in solid-state NMR only in the isotropic phase, this suggests that there is already a π-stacking-driven clustering of TP and TNF in the isotropic phase, and hence incorporation of the TNF molecules into the TP columns is very likely. On the other hand, the ^{1}H MAS spectra of the 50/50 complex exhibit a dramatic reduction of the mobility. This reduction supports the supramolecular "polymer effect" generated by donor−acceptor interactions. In the case of the 100/0 and 90/10 complexes, a significant increase in molecular mobility is observed for temperatures above 40 °C. In the 50/50 complex, the ^{1}H MAS NMR spectra indicate that the molecular mobility is locked-in up to $T = 72$ °C. This temperature corresponds to the onset of the isotropization transition. Quite remarkable is that, in this complex, the alkyl end methyl groups do not show a significant line narrowing with increasing temperature. Thus, even the chain ends of the alkyl chains seem to be frozen.

All these experiments demonstrate that, at the transition from hexagonal columnar to cubic phase, the local packing in the core region is almost unchanged, whereas the outer aliphatic region undergoes significant changes. These results confirm the packing shown in Figure 12 and demonstrate that the mechanism of shape-change from helical pyramidal column to supramolecular sphere is controlled by changes in the packing of the outer aliphatic region of the dendron. At the same time, these experiments demonstrate identical π-stacking of the Tp units in the helical pyramidal column and in the supramolecular sphere that self-organizes in both tetragonal and cubic phases.

Conclusions

The synthesis of two libraries containing 10 triphenylenes dendronized with self-assembling dendrons is reported. A combination of structural and retrostructural analysis demonstrated that dendronized triphenylenes adopt a crown

---

(23) (a) Fréchet, J. M. J.; Tomalia, D. A. Eds. *Dendrimers and other Dendritic Polymers*; Wiley: New York, 2001. (b) Newkome, G. R.; Moorefield, C. N.; Vögtle, F. *Dendrimers and Dendrons*; Wiley-VCH: Weinheim, Germany, 2001.

(24) (a) Lehn, J.-M. *Science* **2002**, *295*, 2400–2403. (b) Lehn, J.-M *Proc. Natl. Acad. Sci. U.S.A.* , *99*, 4763–4768.

(25) (a) Wolffs, M.; George, S. J.; Tomovic, Z.; Meskers, S. C. J.; Schenning, A. P. H. J.; Meijer, E. W. *Angew. Chem., Int. Ed.* **2007**, *46*, 8948–8968. (b) Tsuda, A.; Alam, M. A.; Harada, T.; Yamaguchi, T.; Ishii, N.; Aida, T. *Angew. Chem., Int. Ed.* **2007**, *46*, 8198–8202. (c) Katsonis, N.; Xu, H.; Haak, R. M.; Kudernac, T.; Tomovic, Z.; Georg, S.; der Auweraer, M. V.; Schenning, A. P. H. J.; Meijer, E. W.; Feringa, B. L.; Feyter, S. D. *Angew. Chem., Int. Ed.* **2008**, *47*, 4998–5001. (d) Yashima, E.; Maeda, K.; Furusho, Y. *Acc. Chem. Res.* **2008**, *41*, 1166–1180. (e) Palmans, A. R. A.; Meijer, E. W. *Angew. Chem., Int. Ed.* **2007**, *46*, 8948–8968. (f) Yamamoto, T.; Fukushima, T.; Kosaka, A.; Jin, W.; Yamamoto, Y.; Ishii, N.; Aida, T. *Angew. Chem., Int. Ed.* **2008**, *47*, 1672–1675. (g) Campidelli, S.; Brandmüller, T.; Hirsch, A.; Saez, I. M.; Goodby, J. W.; Deschenaux, R. *Chem. Commun.* **2006**, 4282–4284. (h) Garric, J.; Léjer, J.-M.; Huc, I. *Angew. Chem., Int. Ed.* **2005**, *44*, 1954–1958. (i) Berl, V.; Huc, I.; Khoury, R. G.; Krische, M. J.; Lehn, J.-M. *Nature (London)* **2000**, *407*, 720–723. (j) Pisula, W.; Tomovic, Z.; Watson, M. D.; Müllen, K.; Kussmann, J.; Ochsenfeld, C.; Metzroth, T.; Gauss, J. *J. Phys. Chem. B* **2007**, *111*, 7481–7487.

conformation that mediates, for the first time, the self-assembly of discotic molecules into helical pyramidal columns and in chiral spheres. The helical pyramidal columns self-organize into various hexagonal and rectangular lattices, while the chiral spheres self-organize into cubic and tetragonal periodic arrays and in a quasiperiodic 12-fold liquid quasicrystal. Chiral spheres are created from short fragments of helical pyramidal columns that are spherically distorted. Therefore, their internal helical structure provides a mechanism to amplify chirality and to select the helix sense via a process similar to that used by helical pyramidal columns. Structural parameters that mediate $\pi-\pi$ stacking of triphenylene both in helical pyramidal columns and in chiral spheres were elaborated. In addition, the donor character of triphenylene was used to program the self-assembly process via a new "polymer effect" mediated through donor−acceptor interactions. It is expected that self-assembly of conformationally rigid and flexible dendritic crowns will provide new fundamental and technologically important concepts at the interface between dendrimers,[23] supramolecular chemistry,[24] supramolecular polymer chemistry,[21] supramolecular electronics,[2,11,19c] and supramolecular chirality.[7,9,25] Self-assembly of discotic molecules in solution was extensively investigated.[25a,e,f,i] However, this is the first time that discotic molecules are reported to assemble both in solution and in bulk into supramolecular helical pyramidal columns and chiral spheres via a crown conformation.

Acknowledgment. Financial support by the National Science Foundation (DMR-0548559 and DMR-0520020) and the P. Roy Vagelos Chair at Penn is gratefully acknowledged.

Supporting Information Available: Experimental synthetic procedures with complete spectral, structural, and retrostructural analysis, and complete ref 3c. This material is available free of charge via Internet at http://pubs.acs.org.

JA8094944